



Detailed Design of the High Temperature Heat Pump Laboratory Prototype

PROJECT	CHESTER
PROJECT NO.	764042
DELIVERABLE NO.	3.2
DOCUMENT VERSION	2
DOCUMENT PREPARATION DATE	27/09/2019
RESPONSIBLE PARTNER	UPV
DISSEMINATION LEVEL	Public

Type of Deliverable		
R	Document, Report	X
DEM	Demonstrator, pilot, prototype	
DEC	Websites, patent fillings, videos, etc.	
OTHER		
ETHICS	Ethics requirements	
ORDP	Open Research Data Pilot	



This project has received funding from the European Union's Horizon 2020 research and innovation programme under grant agreement No. 764042.

This deliverable reflects only the author's views and neither Agency nor the Commission are responsible for any use that may be made of the information contained therein.

EC Grant Agreement	No.764042
Project Acronym	CHESTER
Project Title	Compressed Heat Energy Storage for Energy from Renewable sources
Programme	HORIZON 2020
Start Date of Project	01-04-2018
Duration	48 Months

Financial/Administrative Coordinator

Project Coordinator Organization Name	TECNALIA
Address	Parque Tecnológico de Bizkaia C/Astondo, Edificio 700 (Spain)
Phone Numbers	+34 946 430 850
E-mail Address	nora.fernandez@tecnalia.com
Project web-site	www.chester-project.eu

Version Management

Filename	[3.2.: Detailed Design of the High Temperature Heat Pump Laboratory Prototype]		
Author(s)	Abdelrahman Hassan, José-Miguel Corberán, Violeta Sanchez		
Reviewed by	Miguel Ramirez		
Approved by	Felipe Trebilcock		
Revision No.	Date	Author	Modification description
RV 1	05-08-2019	A. Hassan	First version
RV 2	09-09-2019	F. Trebilcock	WP3 leader first review with comments
RV 3	26-09-2019	A. Hassan	Corrected according to the review
RV 4	27-09-2019	M. Ramirez	Final inputs from Tecnalia
RV 5	30-09-2019	A. Hassan	Final version
RV 6	30-09-2019	N. Fernandez	Final formatting

Contents

1.	Introduction.....	8
1.1.	Executive Summary	8
1.2.	Purpose and Scope	8
1.3.	Methodology	8
1.4.	Structure of the document.....	9
1.5.	Relations with other deliverables.....	9
2.	Preliminary Calculations	11
2.1.	Working conditions and restrictions for CHEST prototype	11
2.2.	Refrigerant selection for HTHP.....	11
2.3.	Steady-state EES-CHEST system model	14
2.4.	Compressor selection and performance	15
2.4.1.	Available compressors.....	15
2.4.2.	Compressor selection	20
2.4.3.	Compressor performance.....	21
2.5.	HTHP configuration for experimental campaign.....	21
2.6.	Modeling of heat pump cycles in IMST-ART [®]	22
3.	HTHP Prototype Design	25
3.1.	HTHP Preliminary prototype	25
3.1.1.	Preliminary prototype description	25
3.1.2.	Compressor characterization with R1233zd(E)	26
3.2.	HTHP model for the CHEST prototype.....	28
3.3.	HTHP Components selection and design.....	28
3.3.1.	Condenser.....	29
3.3.2.	Subcooler	31
3.3.3.	Evaporator	31
3.3.4.	Expansion valve	32
3.3.5.	Refrigerant lines	34
3.3.6.	Accessories	35
4.	HTHP Control and Operation Strategies.....	39
4.1.	Instrumentation and control system.....	39
4.1.1.	Main control loop	40
4.1.2.	Evaporator control loop	41
4.1.3.	Subcooler control loop	41
4.1.4.	Compressor's motor cooling control loop.....	42
4.1.5.	Auxiliary control loops.....	42
D3.2 - Detailed Design of the High Temperature Heat Pump Laboratory Prototype		[3]



4.2. Operation control 42

4.3. Start-up procedure 43

4.4. Shut-down procedure..... 44

5. HTHP Prototype Estimated Performance under Steady-state Conditions 45

5.1. Effects of source temperature and compressor speed on the HTHP’s performance 45

5.2. Effect of inlet water temperature to the subcooler (T_{LTWT}) on the HTHP’s performance 48

6. Conclusions..... 51

References 52

Annex..... 53

List of Figures

Figure 1. T-s diagram for: (a) R-718 (wet fluid), (b) R-1233zd(E) (isentropic fluid), and (c) R-1336mzz(Z) (dry fluid).....	12
Figure 2. Work ranges for selected refrigerants and condensation temperature (T_{cond}) in the current work.	13
Figure 3. Schematic of the CHEST system prototype.	14
Figure 4. HTHP with BITZER compressor proposed by Fleckel et al. [9].....	16
Figure 5. Working range for the HTHP proposed by Fleckel et al. [9].....	16
Figure 6. Condensation temperature T_{cond} vs. COP_{HTHP} (left) and $T_{discharge}$ (right) [9].....	17
Figure 7. VHE's single cylinder compressor.....	17
Figure 8. Working envelop for VHE's compressor using R-1336mzz(Z).	18
Figure 9. The prototype DORIN compressor used by Bamigbetan et al. [11].	19
Figure 10. Pressure ratio vs. compressor efficiency as reported by Bamigbetan et al. [11].....	19
Figure 11. Evaporation temperature vs. discharge temperature as reported by Bamigbetan et al. [11].	20
Figure 12. Pressure ratio vs. compressor efficiency (left) and volumetric efficiency (right) for VHE's compressor using R-1336mzz(Z) and R-245fa.	21
Figure 13: HTHP configuration for laboratory testing.....	22
Figure 14. The graphical user interface (GUI) for the HTHP cycle on IMST-ART [®]	24
Figure 15. Schematic diagram of the preliminary HTHP for the testing campaign of the VHE compressor... ..	26
Figure 16. A comparison of VHE's compressor overall efficiency using R-1336mzz(Z) (blue dotted curve) and R-1233zd(E) (orange continues curve)	27
Figure 17. A comparison of VHE's compressor volumetric efficiency using R-1336mzz(Z) (red dotted curve) and R-1233zd(E) (green continues curve)	27
Figure 18. Temperature profiles inside HTHP's condenser for $T_{source,CHEST}= 100$, $T_{melt,PCM}=133$, and $T_{sink,CHEST}=25$ °C.....	29
Figure 19. SWEP B200TH condenser model in IMST-ART [®]	30
Figure 20. Effect of number of plates on SWEP B200TH condenser performance: a) Thermal capacity, b) refrigerant-side pressure drop, c) refrigerant-side HTC, and d) water-side pressure drop.....	30
Figure 21. Temperature profiles inside HTHP's subcooler for $T_{source,CHEST}= 100$, $T_{melt,PCM}=133$, and $T_{sink,CHEST}=25$ °C.....	31
Figure 22. Temperature profiles inside HTHP's evaporator for $T_{source,CHEST}= 100$, $T_{melt,PCM}=133$, and $T_{sink,CHEST}=25$ °C.....	31
Figure 23. Effect of number of plates on SWEP V120TH evaporator performance: a) Thermal capacity, b) refrigerant-side pressure drop, c) refrigerant-side HTC, and d) water-side pressure drop.....	32
Figure 24: Table for selection of the Electronic Expansion Valve.	33
Figure 25: Diagram of CARLY suction accumulator and table of dimensions.	36
Figure 26: Diagram showing the internal parts of the TURBOIL discharge line separators.	36
Figure 27: Diagram of CARLY oil separators and table with dimensions.	37
Figure 28: Table with the dimensions of the Carly liquid receiver and diagram.....	38
Figure 29: Table of dimensions of the selected filter drier.	38
Figure 30. Schematic representation of the HTHP's instrumentation and control system.	39
Figure 31. The HTHP's cycle on P-h diagram for compressor speed of 1500 rpm; and a) $T_{source,HTHP}= 100$ °C, b) $T_{source,HTHP}= 85$ °C, c) $T_{source,HTHP}= 70$ °C, and $T_{source,HTHP}= 55$ °C.	46
Figure 32. Temperature profiles inside HTHP's evaporator for compressor speed of 1500 rpm; and a) $T_{source,HTHP}= 100$ °C, b) $T_{source,HTHP}= 85$ °C, c) $T_{source,HTHP}= 70$ °C, and $T_{source,HTHP}= 55$ °C.	46
Figure 33. Temperature profiles inside HTHP's condenser for compressor speed of 1500 rpm; and a) $T_{source,HTHP}= 100$ °C, b) $T_{source,HTHP}= 85$ °C, c) $T_{source,HTHP}= 70$ °C, and $T_{source,HTHP}= 55$ °C.	47

List of Tables

Table 1. Source and sink temperatures in the different working modes.....	11
Table 2. Properties of selected refrigerants for HTHPs [4]–[6]	12
Table 3. Parametric study for the preliminary HTHP model	28
Table 4. Results from the selection procedure of the MVL661 electronic expansion valve.....	34
Table 5. Refrigerant lines specifications for compressor speed of 500 rpm.....	34
Table 6. Refrigerant lines specifications for compressor speed of 1500 rpm.....	35
Table 7. Instrumentation and control system.....	40
Table 8. Effect of source temperature on the HTHP’s performance for compressor speed of 500 rpm, $T_{\text{melt,PCM}}= 133\text{ °C}$, $T_{\text{LTWT}}=43.8\text{ °C}$, and $T_{\text{HTWT}}=133\text{ °C}$	47
Table 9. Effect of source temperature on the HTHP’s performance for compressor speed of 1000 rpm, $T_{\text{melt,PCM}}= 133\text{ °C}$, $T_{\text{LTWT}}=43.8\text{ °C}$, and $T_{\text{HTWT}}=133\text{ °C}$	48
Table 10. Effect of source temperature on the HTHP’s performance for compressor speed of 1500 rpm, $T_{\text{melt,PCM}}= 133\text{ °C}$, $T_{\text{LTWT}}=43.8\text{ °C}$, and $T_{\text{HTWT}}=133\text{ °C}$	48
Table 11. Effect of inlet water temperature to the subcooler on the HTHP’s performance for compressor speed of 500 rpm, $T_{\text{source,HTHP}}= 85\text{ °C}$, $T_{\text{melt,PCM}}= 133\text{ °C}$, and $T_{\text{HTWT}}=133\text{ °C}$	49
Table 12. Effect of inlet water temperature to the subcooler on the HTHP’s performance for compressor speed of 1000 rpm, $T_{\text{source,HTHP}}= 85\text{ °C}$, $T_{\text{melt,PCM}}= 133\text{ °C}$, and $T_{\text{HTWT}}=133\text{ °C}$	49
Table 13. Effect of inlet water temperature to the subcooler on the HTHP’s performance for compressor speed of 1500 rpm, $T_{\text{source,HTHP}}= 85\text{ °C}$, $T_{\text{melt,PCM}}= 133\text{ °C}$, and $T_{\text{HTWT}}=133\text{ °C}$	50

Glossary, abbreviations and acronyms

CHEST	Compressed Heat Energy Storage
EES	Engineering Equation Solver
GWP	Global Warming Potential
HTHP	High temperature heat pump
HT-TES	High-temperature thermal energy storage
HTWT	high-temperature water tank
LH-TES	Latent heat thermal energy storage
LTWT	Low-temperature water tank
ODP	Ozone Depletion Potential
ORC	Organic Rankine Cycle
P	Pressure
PCM	Phase changing material
PHE	Plate heat exchanger
RES	Renewable energy sources
rpm	Revolutions per minute
SH	Superheat
SH-TES	Sensible heat thermal energy storage
TES	Thermal energy storage
T	Temperature
VHC	Volumetric heating capacity
VHE	Viking Heat Engines

Subscripts

<i>cond</i>	Condensing, condenser
<i>crit</i>	Critical
<i>evap</i>	Evaporation, evaporator
<i>melt</i>	Melting (related to the PCM's melting temperature)
<i>in</i>	Inlet
<i>sc</i>	Subcooler
<i>sink</i>	Chester's heat sink
<i>source</i>	Chester's heat source
<i>w</i>	water

1. Introduction

1.1. Executive Summary

CHESTER project aims to develop an innovative compressed heat energy storage (CHEST) system that allows managing, storing, and discharging of energy using different renewable energy sources (RES) through the combination of electricity and heat sectors [1]. In this system a high temperature heat pump (HTHP) should be utilized to pump the energy from low-temperature sources, such as industrial waste heat, seasonal pit heat storage system, etc., to a high-temperature thermal energy storage (HT-TES) system using the electrical power from RES. In this early stage of the project, the first milestone is to design and test a CHEST system laboratory prototype with 10 kWe capacity. Accordingly, the main goal of the current deliverable is to develop and assess a suitable HTHP that can be integrated to such system.

To do so, firstly the working restrictions for the CHEST prototype system were addressed, and based on this a suitable refrigerant for the HTHP was evaluated and selected, considering its impact on the environment. Secondly, a numerical model of CHEST prototype (EES-CHEST) was developed to identify the individual capacities for HTHP's components and their limits. Thirdly, the process of sizing, selecting and analyzing the different HTHP's components was explained, besides, the control and operation strategies. Finally, to assess the overall performance of the proposed HTHP, different parametric studies were done for different source temperatures, compressor speeds, and inlet water temperatures to the subcooler.

1.2. Purpose and Scope

The objective of the present deliverable is to summarize the design methodology and final characteristics of the HTHP to be integrated in the prototype of the CHEST system. That HTHP prototype will be first tune up, and characterized at Tecnalia and then will be sent to DLR to form part of the complete CHEST system prototype.

This deliverable is a result of Subtask 3.1.3 of the workplan: HTHP design and manufacturing of the laboratory scale prototype, including the description of the design methodology, design requirements, sizing of the main components of the HTHP, and a first assessment of the performance and behavior of the unit, which will be used as a reference to compare with the experimental results of the tuning up and characterization campaign of the prototype, which will be carried out in Tecnalia once the prototype has been manufactured.

1.3. Methodology

First, it has been necessary to analyze and define the HTHP's working conditions, which are also going to be validated with experimental data, taking into consideration the characteristics and limitations of the main components, especially the compressor, and the test rig.

The first design task has been the selection of refrigerant. For this a model of the whole CHESTER model has been employed. The model is programmed in Engineering Equation Solver EES, and allows the calculation of the performance and operation of the entire CHESTER system: HTHP + latent heat storage + sensible heat storage + ORC electric generator. Several refrigerants were studied and the most interesting from the energy point of view, but also considering other issues, as availability, safety, ODP and GWP.

Then, the selection of the high temperature compressor took place, taking into consideration the previously defined operating conditions and the refrigerant that is going to be considered for the HTHP within the CHESTER project. The selection was of course reduced to the few choices available in the market.

The performance of the selected compressor was analyzed in order to characterize its performance and efficiencies. This allowed to develop adequate correlations which were then employed in IMST-ART software in order to model the behavior of the heat pump and assisting the design of the main components.

The heat exchanger design software by SWEP was then used to assist in the selection of the adequate condenser, evaporator and subcooler models, as well for the pre-sizing of the necessary number of plates of each one of the heat exchangers.

The characteristics of the different heat exchangers were introduced in IMST-ART software, which was then use to refine the design of the heat exchangers, and adequately sizing the other components of the unit.

Once that all the main components were selected, the design of the HTHP prototype was completed with the definition of all the auxiliary components (such as piping, valves, liquid receiver, suction-line accumulator, oil separator, etc.), and with the complete definition of the instrumentation, electrical and control system.

Finally, IMST-ART software was employed to estimate the performance and operating conditions of the unit across the range of variation of the independent input parameters.

1.4. Structure of the document

The structure of the document is described in the list of contents. First an introduction, including an executive summary explain the main characteristics of the document. Section 2 describes the preliminary calculations (prior to the design phase), the models that have been employed to estimate the operating conditions and expected performance, and the refrigerant and compressor selection procedures.

Section 3 gives a full description about the design of the unit main components, starting with an explanation about the model of the unit in IMST-ART software, and then describing the design of each of the components.

Section 0 first describes the layout of the unit and the instrumentation that is going to be employed for the experimental characterization of the unit in Tecnia, and then discusses the operation control and the start-up and shut-down procedures, which have been selected initially decided for the testing of the unit.

Finally, section 0 gives a first assessment of the performance and operating conditions of the HTHP by means of the model developed in IMST-ART software.

1.5. Relations with other deliverables

This deliverable has taken information from practically all deliverables coming from WP2, especially, D2.4 [2] detailing the Requirements of individual technologies that form the CHEST system, from D3.1 which deals with the selection and characterization of the oil for the

compressor in the prototype, as well as from the other deliverables D3.3, D3.4 and D3.5 in regard with the interaction with the other components of the CHEST prototype.

The results of this deliverable will be of use for all deliverables in WP3 and WP5 related with the testing of the individual components (WP3) and of the entire prototype (WP5), and it is a previous stage for D3.10, which will try to compile de design specifications for this very special high temperature heat pumps working under very extreme conditions.

2. Preliminary Calculations

2.1. Working conditions and restrictions for CHEST prototype

The working conditions of the CHEST system prototype are set to simulate the six working modes explained in Deliverable 2.4 [2]. The source ($T_{\text{source,CHEST}}$) and sink ($T_{\text{sink,CHEST}}$) temperatures of each mode are listed in Table 1. On the other hand, the melting temperature of phase change material ($T_{\text{melt,PCM}}$) is set to be 133°C, which is the temperature of the latent heat thermal energy storage (LH-TES) system.

Table 1. Source and sink temperatures in the different working modes

Variable	Mode 1	Mode 2	Mode 3	Mode 4	Mode 5	Mode 6
$T_{\text{source,CHEST}}$	80	80	100	100	60	40
$T_{\text{sink,CHEST}}$	40	10	40	10	60	60

Thus, working conditions for the HTHP are, initially, 133 °C for HTHP’s sink (temperature of LH-TES system) and from 40 °C to 100 °C for HTHP’s source (CHEST’s system evaporator). However, low source temperatures will lead to high pressure ratios and very low volumetric and compressor efficiencies, then, Mode 6, with a HTHP’s source temperature of 40°C, implies technical difficulties and cannot be simulated in the laboratory prototype. For that reason, the minimum HTHP’s source temperature will be 55 °C.

In this way, HTHP’s working conditions for the laboratory prototype are:

- $T_{\text{source,HTHP}} = T_{\text{source,CHEST}} = 55\text{-}100$ °C.
- $T_{\text{sink,HTHP}} = T_{\text{melt,PCM}} = 133$ °C (fixed).

It is worth mentioning that the nominal point for the CHEST prototype was defined as follows:

- $T_{\text{source,CHEST}} = 85$ °C.
- Evaporator’s water-side temperature lift ($\Delta T_{\text{w,evap}}$)= 5 K.
- $T_{\text{sink,CHEST}} = 25$ °C.
- Condenser’s water-side temperature lift ($\Delta T_{\text{w,cond}}$)= 5 K.

2.2. Refrigerant selection for HTHP

Selection of the proper refrigerant is a crucial decision for designing HTHPs. One important aspect to choose a proper one is the required degree of superheat (SH) after evaporation. Low SH values could result in wet compression, while high values could decrease the evaporation temperature and affect significantly the system performance. Based on this, the refrigerants could be classified into three groups based on the slope of saturated vapor curve on T-s diagram (dT/ds). The negative slope refrigerants are called “wet fluids”, the positive slope ones are called “dry fluids”, and semi-vertical slope refrigerants are called “isentropic fluids” [3]. Figure 1 presents a comparison of the three type of curves showing one representative refrigerant for each case.

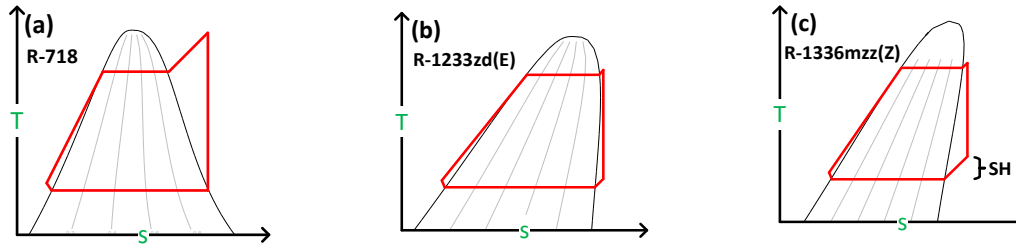


Figure 1. T-s diagram for: (a) R-718 (wet fluid), (b) R-1233zd(E) (isentropic fluid), and (c) R-1336mzz(Z) (dry fluid)

As it can be seen from the previous figure, wet fluids will not necessarily require a superheating at the evaporator's outlet port, while dry fluids need a very high degree of SH to prevent wet compression operation. On the other hand, the isentropic fluids need a moderate degree of SH that could be done inside the evaporator without side effects on the system performance.

Other desirable criteria of the refrigerants used especially in HTHPs applications are: zero ozone depletion potential (ODP=0); very low global warming potential (GWP<10); non-toxic; no or low flammability; high critical temperature ($T_{crit}>145$ °C) allowing for subcritical applications; low critical pressure ($P_{crit}<3$ MPa). Regarding the criteria discussed, Table 2 lists a sample of different refrigerants that could be employed in HTHPs applications.

Table 2. Properties of selected refrigerants for HTHPs [4]–[6]

Group	Refrigerant	Type	T_{crit} (°C)	P_{crit} (MPa)	NBP ^a (°C)	ODP (-)	GWP (-)	SG ^b
Wet (W)	R-718 (water)	Natural	373.95	2.206	100.0	0	0	A1
	Acetone	HC ^c	235.0	4.7	56.0	0	<10	n.a.
Dry (D)	R-1336mzz(Z)	HFO ^d	171.3	2.9	33.4	0	2	A1
	R-365mfc	HFC ^e	186.85	3.266	40.2	0	804	A2
Isentropic (S)	R-1233zd(E)	HCFO^f	166.5	3.62	18.7	0.0003	<1	A1
	R-245fa	HFC	154.01	3.65	15.1	0	858	B1
	Butene	HC	146.15	4.0	-6.3	0	<10	n.a.

^aNBP: normal boiling point at 0.1013 MPa; ^bSG: safety group [7]; ^cHC: hydrocarbons; ^dHFO: hydrofluoroolefins; ^eHFC: hydrofluorocarbons; ^fHCFO: hydrochlorofluoroolefins.

Figure 2 shows the work ranges for refrigerants listed in Table 2. The work range is defined as the difference between critical temperature (T_{crit}) and normal boiling point (NBP). This gives an idea for the ability of refrigerant to reach a certain condensation temperature (T_{cond}) and its proximity to the critical point. In the present analysis, the value of T_{cond} is assumed to be 5 Kelvin higher than the PCM's melting temperature, in this case it equals to 138 °C, as seen in Figure 2.

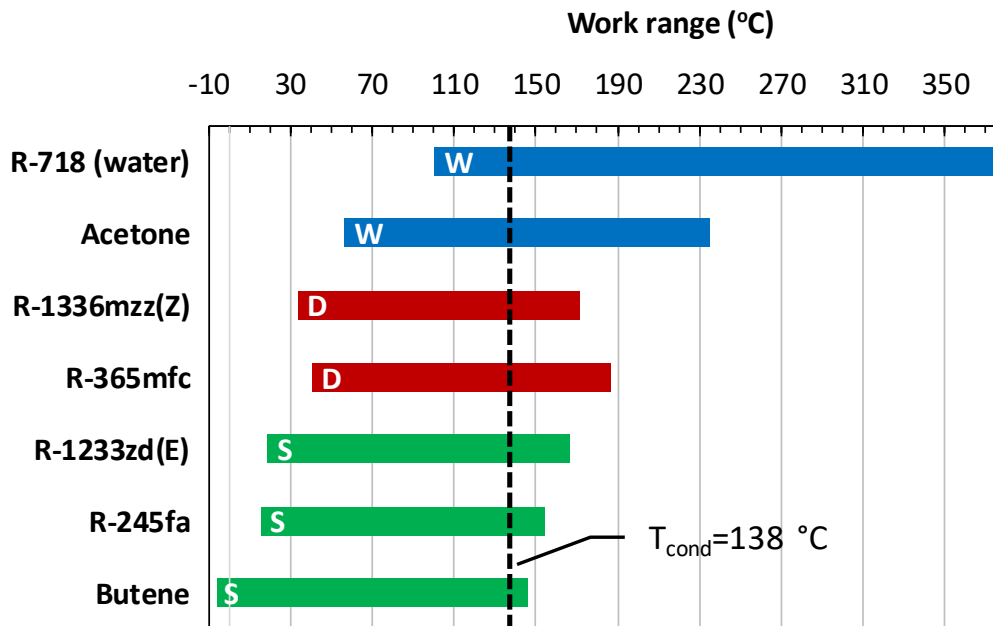


Figure 2. Work ranges for selected refrigerants and condensation temperature (T_{cond}) in the current work.

Apagaus et al. [4] reported that for subcritical HTHPs, the difference between T_{crit} and T_{cond} should be between 10 and 15 K to ensure a reasonable performance. Regarding this condition, it can be noticed that the R-718 (water), Acetone, and R-365mfc are the only refrigerants that have a sufficient difference between critical and condensation temperatures. The wet fluids, Water and Acetone, has many desirable properties, such as very high latent heat and T_{crit} ; however, because of its low vapor density it requires complicated multi-stage compression cycles with intercooling to cope the high values of pressure ratio and discharge temperature. Also, they have a very high NBP values that means that the HTHP's evaporator could work under a negative pressure, especially for a source temperature lower than 60 °C, subsequently, the air can infiltrate easily to the cycle at the presence of any leakage. Due to these reasons, Water and Acetone have been excluded from the analysis.

The dry fluids, R-1336mzz(Z) and R-365mfc, require high SH values to prevent the wet compression. This significantly decreases the evaporation temperature and, consequently, the system performance. To prevent the performance degradation, it is very important to employ an external superheater [8], and such type of equipment cannot be employed in the current CHEST configuration. Therefore, they were also excluded.

From the previous analysis, we can conclude that the most suitable refrigerants to be considered for the CHEST system HTHP prototype are the ones with an isentropic behavior. They have very desirable features such as; high volumetric heating capacity (VHC) values, low discharge temperatures, low pressure ratios, and they require low values of SH, compared to wet and dry fluids [8]. Based on this, R-1233zd(E) was selected as the working fluid for the HTHP employed in the CHEST prototype. R-1233zd(E) is a nonflammable and nontoxic refrigerant. It has very low GWP value, besides, it has a high critical temperature (166.5 °C) which allows the HTHP to work under subcritical conditions with high COP values.

2.3. Steady-state EES-CHEST system model

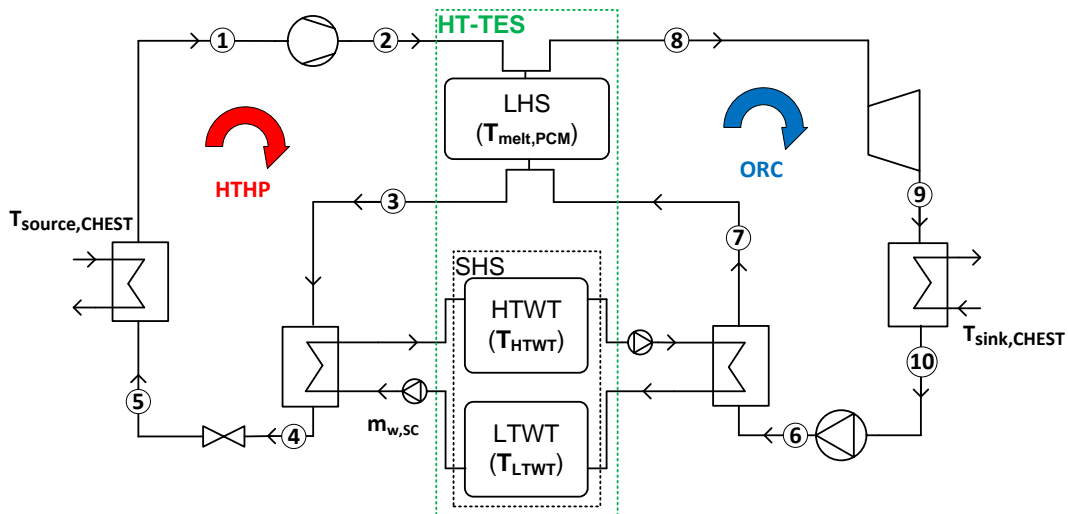


Figure 3. Schematic of the CHEST system prototype.

Figure 3 shows a schematic representation of the CHEST system prototype. The left-hand-cycle represents the HTHP (charging cycle) which is coupled to the organic Rankine cycle (ORC) (right-hand-cycle or discharging cycle) with a high-temperature thermal energy storage (HT-TES) system. It can be noticed that the HT-TES system is divided into two sub-systems: latent heat thermal energy storage (LH-TES) system and sensible heat thermal energy storage (SH-TES) system. The SH-TES system comprises two water tanks where the water is circulated in between. The HTHP's subcooler (3→4) is used to increase the water temperature in the charging cycle and to store sensible heat in the high-temperature water tank (HTWT). In the discharging cycle, the ORC's preheater (6→7) uses the stored sensible heat to preheat the refrigerant before entering the LH-TES. The outlet water from the preheater is circulated again to the low-temperature water tank (LTWT).

The Engineering Equation Solver [5] (EES) simulation program was used to model the proposed CHEST system shown in Figure 3. This program has many desirable features such as modeling simplicity, many methods for system optimization, thermo-physical properties database for vast number of refrigerants and secondary fluids, and detailed presentation of thermodynamic cycles on P-h and T-s diagrams.

In the EES-CHEST model, the HTHP and ORC are coupled to obtain the optimum temperature for the low-temperature water tank (T_{LTWT}) as a function of the source and sink temperatures, and water-side temperature lifts.

This model is considered to be a primary step to size the HTHP components and predict the global performance of the CHEST system prototype.

To do so, the following modelling assumptions have been adopted:

- The system works in steady-state conditions.
- R-1233zd(E) is the working fluid for both HTHP and ORC.
- No heat losses in the high- and low-temperature water tanks.
- No glide in the melting temperature of the PCM ($T_{melt} = 133$ °C).
- All the heat (sensible and latent) stored during charging cycle, is consumed by discharging cycle with the same ratio between latent and sensible heat.

- The inlet to the HTHP's subcooler and outlet from the ORC's preheater is always saturated liquid.

2.4. Compressor selection and performance

2.4.1. Available compressors

For capacities around some MWs and larger, what would be the case of the Full CHEST system, the best compressor technology will be radial turbomachine, i.e. turbocompressor technology. However, the CHEST prototype would be much smaller, heating capacity around 40 kW, with compressor consumption around 10 kWe, since it must be fully tested at the laboratory.

Turbomachinery cannot be used in general for small capacities since the passage sections would be too small and friction would become a very important loss. Additionally, the speeds should be very high complicating the electricity generation. Additionally, the development of efficient turbocompressor technology is very expensive, and must be adapted to the application characteristics. Currently there is no commercially available solution for small size.

In some references, scroll or screw compressors are found as expanders. Those technologies should be of course able to work as compressors. However, the fact that we are going to work with temperatures probably above 150 °C makes lubrication very difficult. Lubrication is essential to avoid rapid wearing where metal to metal contact could appear. However, lubrication, additionally must perform as well the role of sealing between high- and low-pressure parts along the compression process. Although piston compressors are more critical for lubrication from the point of view of the wearing on the contact between the rings and the cylinder walls, they are more effective in keeping the sealing between the vapor compressed above the piston and the crankcase. On the other side, screw can keep an easier and more effective lubrication but greatly rely on the sealing by the lubricant. Scroll compressors requirements, concerning lubrication, are very strong for both roles, avoiding wearing as well as for keeping the sealing.

Therefore, considering, both the size of the prototype and the difficulties of the lubrication with the high operation temperatures, the recommended compressor technology for the prototype is piston compressor.

After a thoroughly search of the literature, the following piston compressors have been found to have reached high discharge temperatures and have been used in heat pumps for high temperature applications: Bitzer [9], Viking Heat Engines [10], and Dorin [11].

a) BITZER

In the presentation by Fleckel et al. [9] it is stated that the compressor used within the analysis is a BITZER semi-hermetic reciprocating compressor with external frequency inverter (ABB). Nominal heating capacity at $T_{\text{cond}}=100$ °C and $T_{\text{evap}}=65$ °C is 12 kW. The heat pump prototype with the mentioned compressor on the top can be seen in Figure 4.



Figure 4. HTHP with BITZER compressor proposed by Fleckel et al. [9].

The compressor was tested for a range of operating conditions with refrigerant R1336mzz-Z, as shown in Figure 5.

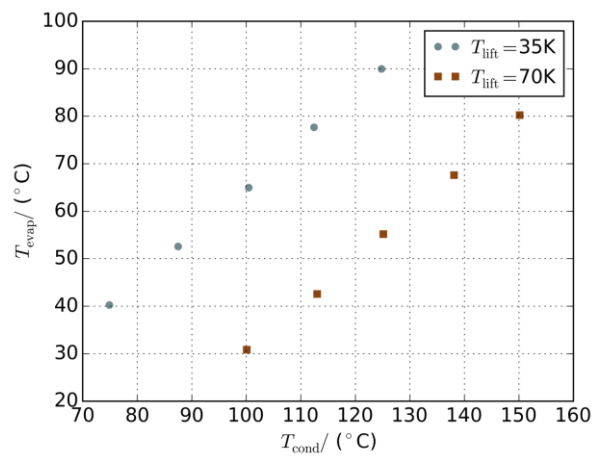


Figure 5. Working range for the HTHP proposed by Fleckel et al. [9].

The heat pump showed a considerably high COP depending on the source temperature, and discharge temperatures were relatively moderate, as demonstrated in Figure 6.

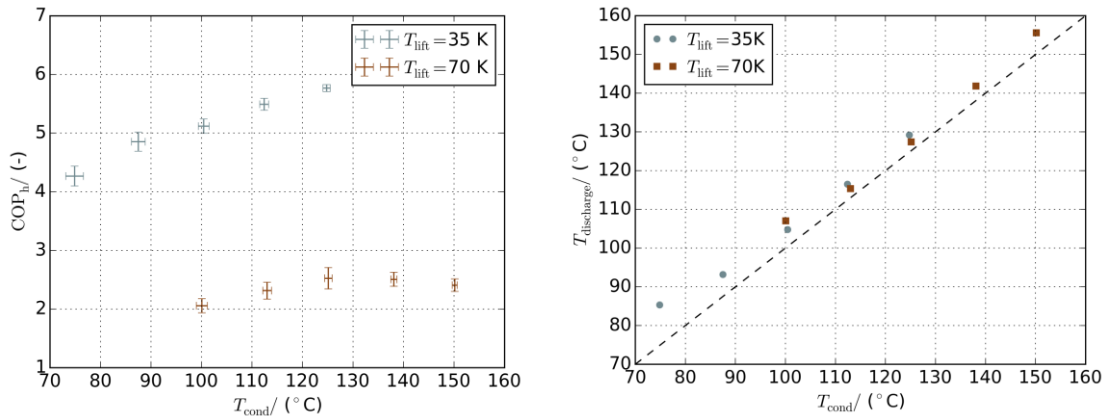


Figure 6. Condensation temperature T_{cond} vs. COP_{HTHP} (left) and $T_{discharge}$ (right) [9].

b) VIKING HEAT ENGINES (VHE)

Viking Heat Engines (VHE) is commercializing the heat pump, 'HeatBooster' with the highest output temperature in the market [10]. They offer a range of heat pumps from 50 to 200 kW_{th} per unit, which produce high-temperature heat up to 165 °C.

The compressor they employ is a 'heavy-duty piston-type compressor developed in collaboration with AVL Schrick': HBC 511. Figure 7 shows a picture of their single cylinder compressor.



Figure 7. VHE's single cylinder compressor.

The compressor has been engineered to operate at very high internal temperatures and pressures. It's compatible with all common refrigerants of the 3rd and 4th generations (e.g. HFOs). The compressor has an efficient integrated synchronous motor (PMM), and reaches a high isentropic and volumetric efficiency over a broad range of operating conditions by utilizing a

variable speed operation. The single cylinder compressor has a displacement of 511 cm³, and the compressor speed can be varied from 500 rpm to 1500 rpm.

The operating envelope of HBC 511 working with R-1336mzz(Z) is shown in Figure 8, indicating a maximum condensation temperature of 160 °C.

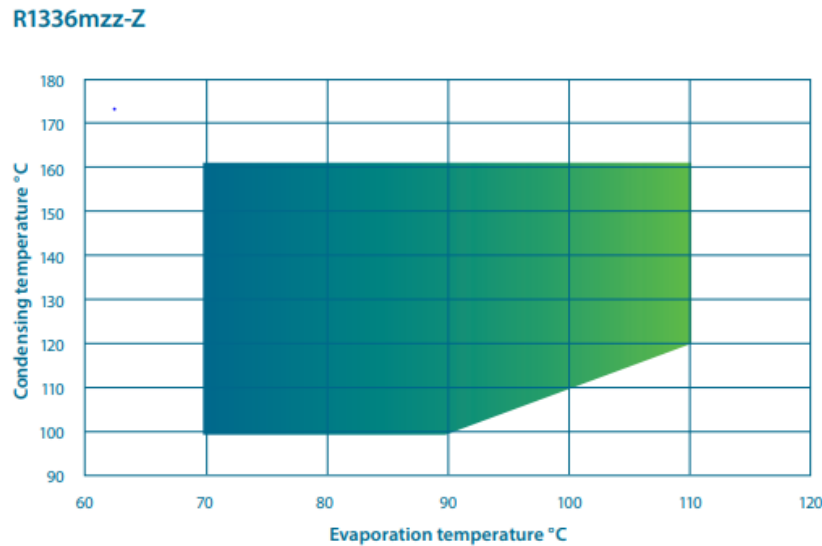


Figure 8. Working envelop for VHE's compressor using R-1336mzz(Z).

c) DORIN

As stated in Bamigbetan et al. [11], the compressor is a single-stage semi-hermetic piston compressor with butane as the working fluid, modified for high temperature operation. The prototype compressor has a displacement of 48.82 m³/h at 50 Hz. It is a one-stage semi-hermetic 4 – cylinder piston compressor designed for operation in an explosive atmosphere. The compressor is installed with an internal crankcase heater, an oil sight glass and is equipped with an external oil separator and oil return valve. The compressor is modified with an external manifold at the discharge connection point to effectively manage the high temperatures. The electric motor of the compressor is sized 25 % larger than would be typical for the compressor size. This will reduce heat generation at high loads on the electric motor. It will also allow better flexibility of the compressor for the varying test conditions. The compressor has a thermal protection set at 140 °C with a special discharge temperature sensor at 160 °C. A high-pressure switch is installed for safety at 28.6 bar. An image of the prototype compressor is shown Figure 9.



Figure 9. The prototype DORIN compressor used by Bamigbetan et al. [11].

Compressor efficiencies, reported by the authors, are shown in Figure 10, being considerably high.

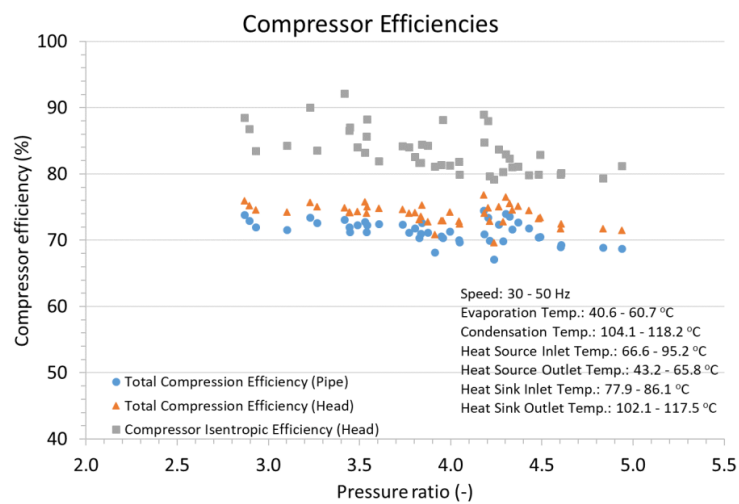


Figure 10. Pressure ratio vs. compressor efficiency as reported by Bamigbetan et al. [11].

The corresponding discharge temperatures are shown in Figure 11.

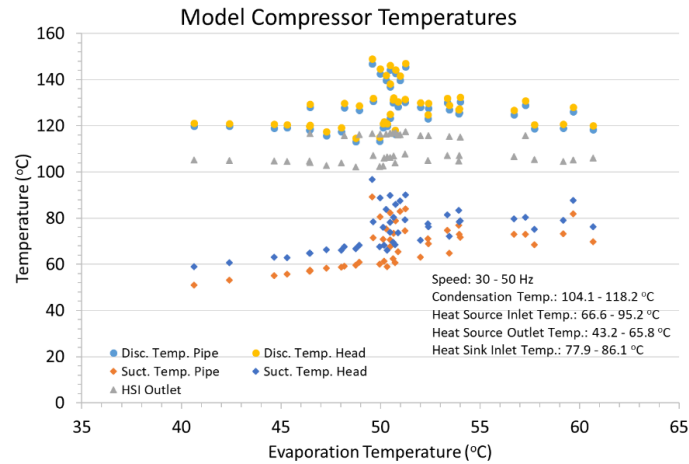


Figure 11. Evaporation temperature vs. discharge temperature as reported by Bamigbetan et al. [11].

2.4.2. Compressor selection

All mentioned manufacturers were contacted in order to know the available sizes and characteristics of their compressors, and their suitability to work with the refrigerants we were considering as the best options for the CHESTER heat pump prototype.

HBC 511 compressor by VHE was clearly the most advanced compressor for this kind of application. In fact, it is a new development especially design for high temperature applications. Therefore, it was decided that HBC 511 will be the compressor to be employed in the CHESTER heat pump prototype. HBC 511 single cylinder compressor has exactly the displacement adequate to reach the heat output defined in the project proposal for the prototype at 1500 rpm, with the advantage that the heat capacity can be continuously modulated by varying the compressor speed from 500 to 1500 rpm.

DORIN also offered one compressor, similar to the one they had employed in the above referred research study, and therefore it will be tested as well in a second phase of the heat pump prototype tests at Tecnalia's laboratory. The 4-cylinder compressor selected has a total displacement similar to the HBC 511 single cylinder at 1500 rpm.

VHE is going to provide advice to the project consortium about the possible adaptations required to employ the selected refrigerant with HBC 511 since R-1233zd(E) has never been tested in their lab. For this reason, a short experimental campaign of HBC 511 with R-1233zd(E) has been carried out by Tecnalia, also with the objective of checking the good operation of the instrumentation and the compressor testing layout.

Given that the application is going to reach very high condensation temperatures and high evaporation temperatures with a new refrigerant, the lubrication of the compressor becomes a critical task. This is the reason, why a whole subtask of CHESTER project has been dedicated to find out the most adequate oil, and lubrication operation, including preheating of the oil prior to the start-up and maybe cooling of oil during operation. The results of this study can be found in D3.1. of the Chester project.

2.4.3. Compressor performance

As commented above, VHE has never tested HBC 511 compressor with the selected refrigerant, therefore there was no specific information about the adequate operation envelope for R1233zdE, and no estimation of the expected performance. In order to be able to solve this, VHE provided with available experimental results for other refrigerants, namely: R-245fa and R-1336mzz(Z). Universitat Politècnica de València (UPV) team employed this information to estimate the volumetric efficiency, the compressor efficiency and the rate of heat losses to the ambient, which are the three parameters that are necessary in order to estimate the performance of the compressor. This information was adequately fitted to standard polynomials in order to be able to evaluate these parameters in IMST-ART[®] software (which is described in the Sub-section 2.6), and in this way proceed to assist the design of the other HTHP's components. The identified volumetric and compressor efficiencies for VHE's compressor are illustrated in Figure 12.

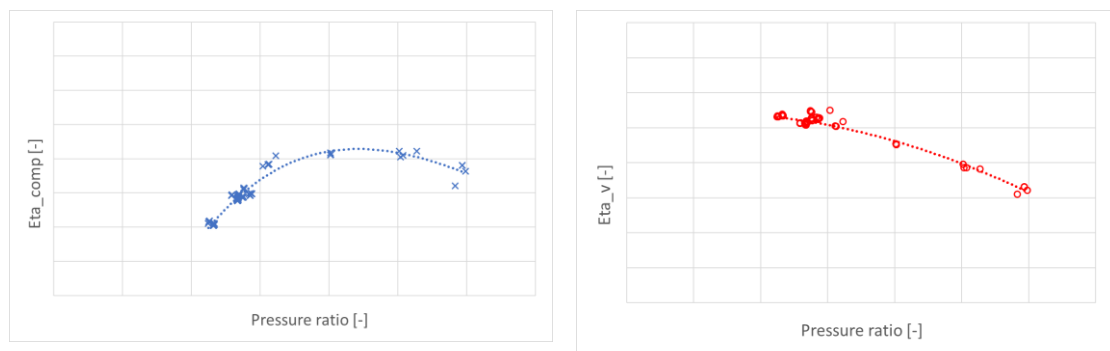


Figure 12. Pressure ratio vs. compressor efficiency (left) and volumetric efficiency (right) for VHE's compressor using R-1336mzz(Z) and R-245fa.

In order to validate the prediction of the compressor performance for the selected refrigerant, the correlations were compared with the preliminary experimental evaluation of performance made by Tecnia, which is described in Section 3.1.2. The validation was considered satisfactory given the uncertainty of the measurements in these preliminary tests, and the reduced number of tests. Therefore, the developed correlations have been employed to assist the design of the heat pump components.

2.5. HTHP configuration for experimental campaign

Figure 13 shows the schematic of the HTHP configuration for laboratory testing (the one that is sized and evaluated in the current deliverable). It can be noticed that a brazed-plate heat exchanger (BPHE) is employed as condenser in this configuration; however, to integrate the HTHP to the CHEST system prototype the condenser will be removed and the refrigerant will condensate directly inside a bundle of tubes integrated within the LHS. Many accessories have also been considered such as oil separator, suction-line accumulator, and liquid receiver to test their effects on the system performance. Mainly, the suction-line accumulator is used to prevent the excess superheat for wet and isentropic refrigerants, while the liquid receiver is adopted to ensure a saturated liquid at the inlet of subcooler. Each heat exchanger has its variable speed pump to control the flow rate of water and the total capacity.

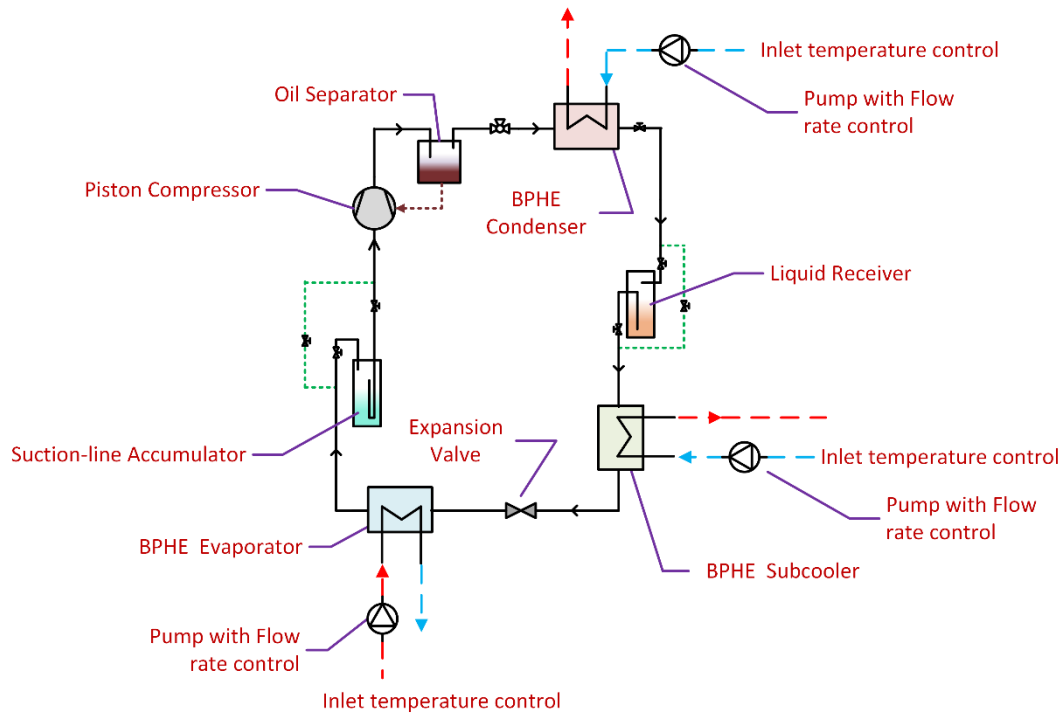


Figure 13: HTHP configuration for laboratory testing

2.6. Modeling of heat pump cycles in IMST-ART[®]

IMST-ART[®] [12] is a commercial software developed by UPV, which allows the estimation of the performance of refrigeration equipment/ heat pumps following the vapor compression cycle. It is based on advanced and detailed mathematical models of the different components of the unit and it is usually employed to assist the design of that kind of equipment. IMST-ART has been fully validated in a large number of experimental studies with different systems and applications, and have proved to provide very accurate performance predictions, around $\pm 5\%$ of the measured values. IMST-ART[®] software was presented for the first time at Corberán and González [13]. For a full description of its characteristics and capabilities, please visit: <http://www.imst-art.com/>.

The global model of the system is divided into sub-models: compressor, heat exchangers, expansion device, accessories, and piping. Each sub-model involves a series of non-linear equations and in the case of the heat exchangers, the solution of a system of ODEs, which is discretized with a finite volume technique. Then, the sub-models are coupled to form a global model of the heat pump. The global set of equations forms a complex system of non-linear equations AEs and DAEs, which is solved globally by a Newton-like solver.

The independent variables chosen for the global set of equations are pressure and enthalpy at each inlet and outlet point. This choice assures a smooth variation of the variables, not given by other choices like temperature or quality.

Calculation of the refrigerant's thermodynamic and transport properties are obtained from REFPROP [5] subroutines for each refrigerant considered within the analysis. The corresponding properties are then conveniently stored in a refrigerant data library. The required properties during the simulations are estimated by interpolation from the corresponding data file.

Additionally, built-in tables allow the calculation of the properties of any usual secondary fluid, i.e. dry air, humid air, water and common brines.

The global system of equations is solved using a standard solver based on the MINPACK subroutine HYBRD1, which uses a modification of M.J.D. Powell's hybrid algorithm. The program continuously surveys the convergence of the method and a special strategy to find appropriate initial solutions and also to carefully bound variables and functions have been worked out. The result of all this is an extremely robust and fast software.

The modelling of the heat exchangers follows a detailed finite volume approach. The numerical method employed is called SEWTLE [14] (for Semi Explicit method for Wall Temperature Linked Equations). Basically, this method is based on an iterative solution procedure. First a guess is made about the wall temperature distribution; then the governing equations for the fluid flows are solved in an explicit manner leading to the estimation of the outlet conditions at every fluid cell, from the values at the inlet of the HE and the assumed values of the wall temperature field. Once the solution of the fluid properties is got at every fluid cell, then the wall temperature at every wall cell is estimated from the balance of the heat transferred across it. This procedure is repeated until convergence is reached. The numerical scheme developed for the calculation of the temperature at every wall cell is also explicit, so that the global strategy consists in an iterative series of explicit calculation steps. For further description please refer to Corberán et al. [14]. Dedicated empirically adjusted correlations are employed for the evaporation and condensation heat transfer coefficients in the BPHEs.

The modelling of the compressor is usually done by the three empirical parameters: volumetric efficiency, compressor efficiency, and the heat losses (fraction of power input which is lost to the environment from the outer shell of the compressor) which are determined from the actual compressor performance map. For standard commercial compressors it is also possible to directly input the AHRI polynomial coefficients provided by the manufacturers for the refrigerant mass flow rate and power input. The manufacturers do not provide information about the discharge temperature or heat losses; hence, the heat losses fraction must be still estimated from experience.

Once the compressor was selected, and some experimental performance data was available, the volumetric efficiency, the compressor efficiency and the heat losses fraction for the VHE compressor were developed, as described in Sub-section 2.4. These data, in form of correlations was then input in IMST-ART[®], as well as other initial data about the heat exchangers, in order to make a first estimation of the thermodynamic conditions at the inlet and outlet of each of the components. The model in IMST-ART[®] was then employed for the selection and pre-sizing of the main components of the unit as it will be described in the following section. Figure 14 shows the input screen of IMST-ART[®] model for the CHEST HTHP prototype.

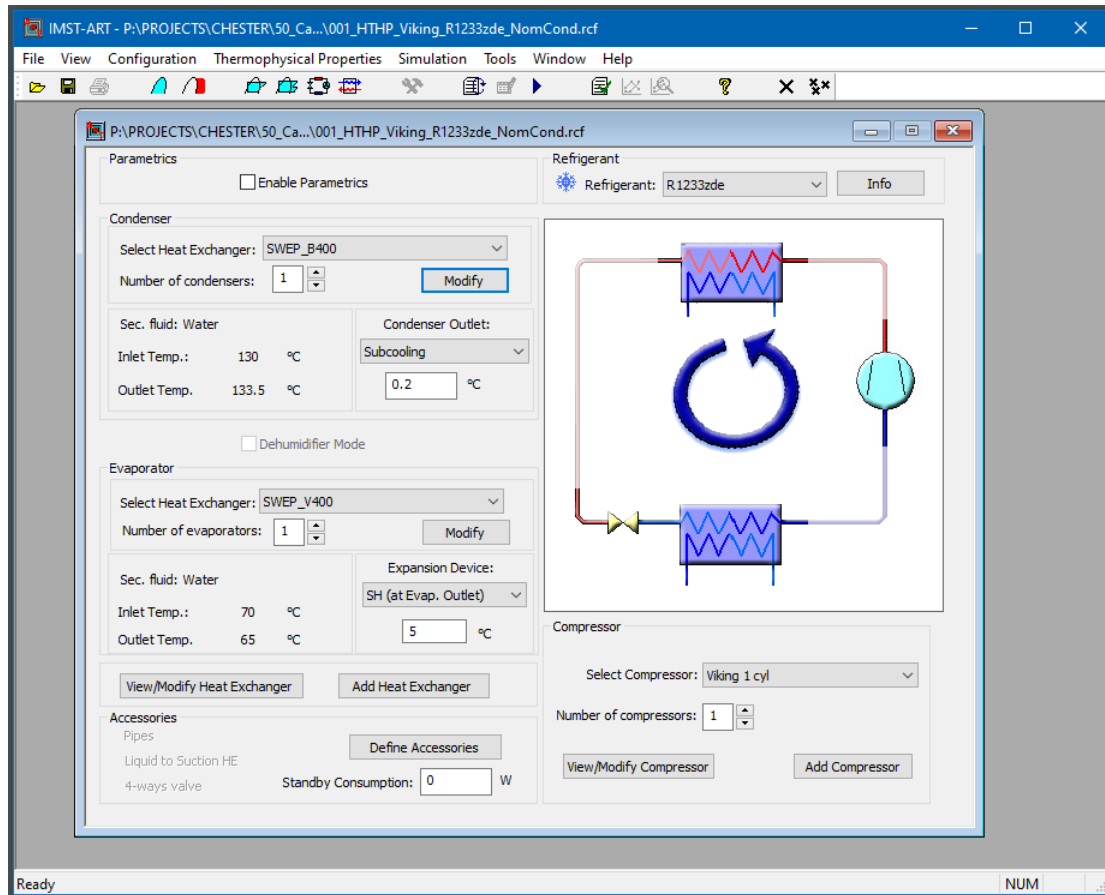


Figure 14. The graphical user interface (GUI) for the HTHP cycle on IMST-ART®.

3. HTHP Prototype Design

3.1. HTHP Preliminary prototype

3.1.1. Preliminary prototype description

The working fluid selected for the CHESTER prototype is the R-1233zdE, but the VHE compressor manufacturer could not provide any experimental results of its performance with this fluid. However, they provided experimental results using the working fluids R-245fa and R-1336mzZ. For this study, the data of these two fluids was insufficient to deliver solid assumptions of the compressor performance at the CHESTER operating conditions. Therefore, the compressor was mounted in the HTHP testing rig of TECNALIA to perform a testing campaign. The results of the compressor testing provide useful data needed to validate the simulations.

The HTHP preliminary prototype consists of the compressor, two evaporators, a condenser, a subcooler, the expansion device, a liquid receiver, the auxiliary components and all monitoring devices. The configuration of the HTHP is single loop with a subcooler and two evaporators connected in parallel as presented in Figure 15. Vapor is compressed by the VHE compressor and discharged to the condenser. At the discharge line a discharge muffler has been installed to reduce the pulsations caused by the single cylinder compressor. Pulsations may cause noise and vibration through all the pipe work and the structure affecting some measurements of sensors and the integrity of the refrigeration loop.

The condenser transfers heat from the vapor to the water which is the secondary fluid. The refrigerant is condensed and directed to the liquid receiver where a liquid level is maintained. The liquid refrigerant passes through the Coriolis flow meter and enters an additional heat exchanger (subcooler) which increases the subcooling degree of the fluid. Heat from the high-pressure liquid is transferred to the subcooler's water loop. High pressure subcooled liquid passes through the filter, the solenoid valve, and the sight glass to enter into the expansion device.

The electronic expansion valve (EEV) reduces the pressure of the fluid and the low-pressure liquid is sent to the two evaporators in a parallel configuration. The liquid refrigerant is evaporated by the heat transferred from the source water loop. The vapor is superheated according to a setpoint which is maintained by the opening degree of the EEV. The vapor exiting the evaporators passes through a suction line separator to avoid liquid droplets entering the suction line of the compressor. The vapor is then compressed by the single-piston compressor and the cycle

The compressor requires cooling and is achieved by an additional closed water loop. It consists of a water pump, a fan coil and an expansion vessel. During the compressor operation the water pump can operate at three different speeds depending on the cooling demand of the compressor. The speed of the compressor is controlled by a SIEMENS inverter which has been provided by VHE.

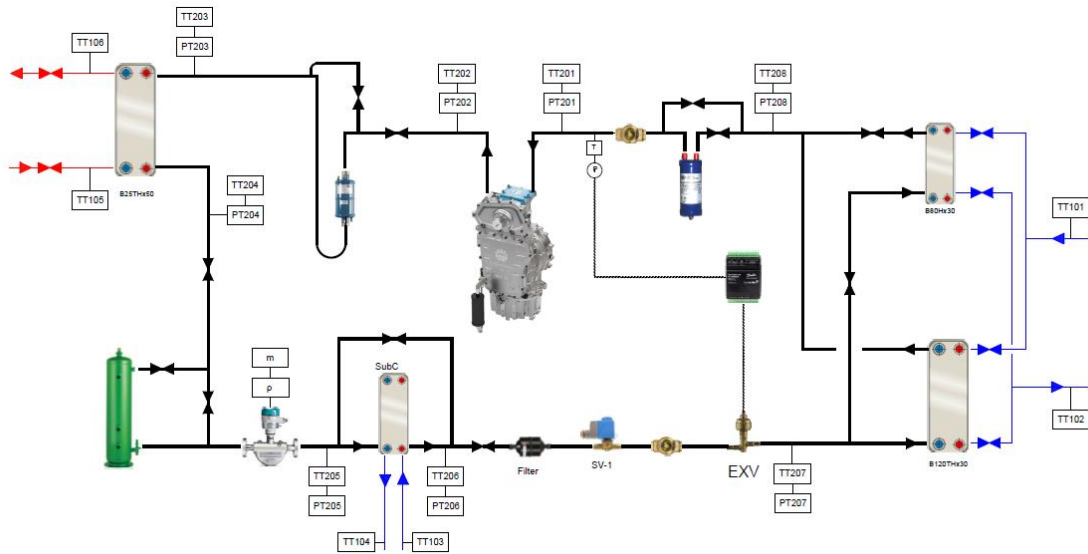


Figure 15. Schematic diagram of the preliminary HTHP for the testing campaign of the VHE compressor.

The preliminary prototype is equipped with monitoring devices measuring temperature, pressure, flow rates and power consumption. In the refrigerant cycle temperatures and pressures have been monitored at the inlet and outlet of heat exchangers and the compressor. The flow rate was monitored in the liquid line using a Coriolis type flow meter.

In the water loops the temperature is measured at the inlet and outlet of all heat exchangers. In addition, the flow rate is measured in each water loop.

The data acquisition system consists of a data logger of Delphin Expert Logger, the RS485 cable, the PROFIBUS extension slaves. All data is monitored and saved in the main laboratory computer in datalogging sequence of 1 second.

3.1.2. Compressor characterization with R1233zd(E)

The preliminary HTHP prototype has been tested in different operation conditions. The characterization of the VHE compressor consisted in series of testing of source water temperatures of 72, 82, 92 and 105 °C. The water sink temperature was maintained during all tests at 133.5 °C. The water flow rate in the evaporator, condenser and subcooler was maintained stable during all tests.

For each source temperature operating condition, the compressor was also tested at different motor speeds, they were 1000, 1230 and 1500 rpm. The flow rate of the cooling water entering the compressor was controlled according to the motor temperature and the evaporating temperature.

The data collected of the testing campaign was filtered and analyzed. The calculated COP of the preliminary HTHP ranged in between 3.8 to 7.16 for all the tests.

A comparison between the volumetric and compressor efficiencies estimated from the experiments carried out with R-1233zd(E) at 1500 rpm (4 orange points in Figure 16 and green points in Figure 17), with the values estimated from the information provided by VHE when considering other refrigerants (Section 2.4.3), is shown in Figure 16 and Figure 17.

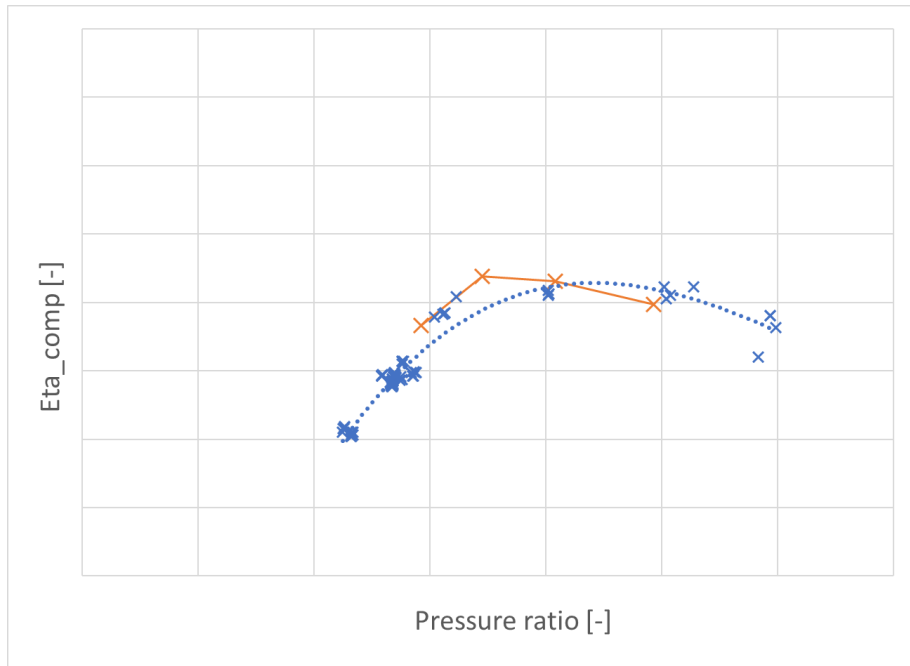


Figure 16. A comparison of VHE’s compressor overall efficiency using R-1336mzz(Z) (blue dotted curve) and R-1233zd(E) (orange continues curve)

As it can be observed, the compressor efficiencies calculated from the experimental results with R-1233zd(E) are close to the ones estimated from the experiments with other refrigerants, with slightly higher values. However, given that, only 4 points are available and the difficulties in measuring, mainly due to high vibration, it is recommendable to continue using the correlation developed originally from VHE data since it is based on a much higher number of experiments. If the efficiencies in the end are better than the estimated ones, as the preliminary data seem to indicate, the design will be on the conservative side.

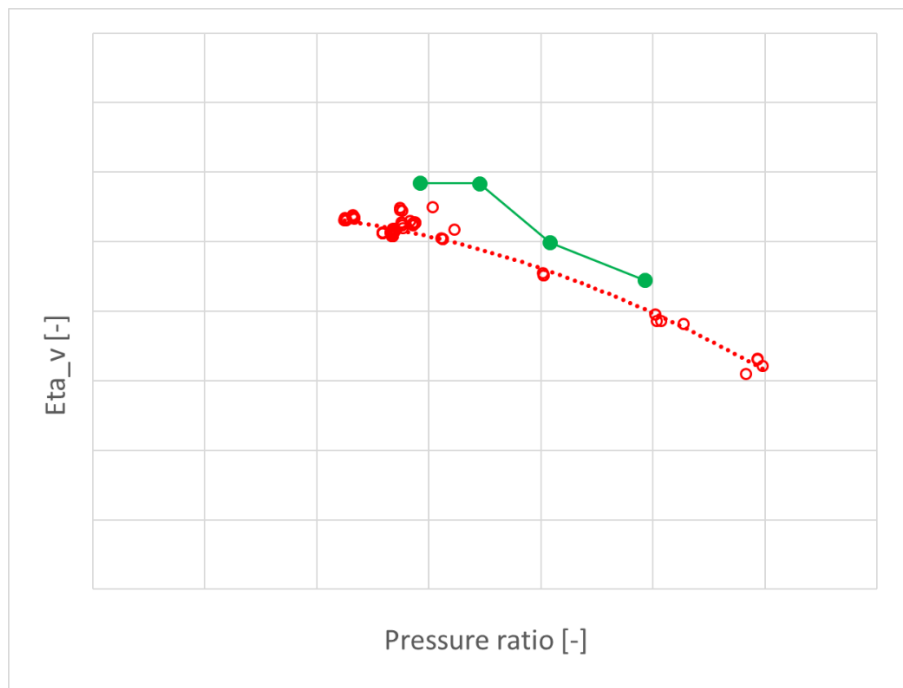


Figure 17. A comparison of VHE’s compressor volumetric efficiency using R-1336mzz(Z) (red dotted curve) and R-1233zd(E) (green continues curve)

3.2. HTHP model for the CHEST prototype

As mentioned before, The HTHP model for the CHEST prototype was developed using IMST-ART[®] simulation tool, for more details about the program please refer to Sub-section 2.6. As a preliminary design step, the HTHP model was based on the plate heat exchangers proposed for HeatBooster heat pump but the number of plates for the condenser and evaporator was reduced to coincide with a one-cylinder compressor and the heat loads required for CHEST system prototype.

The compressor was defined inside the IMST-ART[®] by the compressor displacement [cm³], oil volume [dm³], compressor speed [rpm], oil circulation rate [%], heat losses [%], and external inverter efficiency [%]. The overall compressor and volumetric efficiencies were introduced as polynomials based on the HeatBooster experimental data for R-1336mzz(Z) (Section 2.4.3) and Tecnalia's test bench for R-1233zd(E) (Sub-section 3.1.2).

A parametric study was done for $T_{source,CHEST}$ ranges between 40 and 100 °C, while the inlet water temperature to condenser was kept constant at 133 °C, with high mass flow rate, to resemble the behavior of condensation process inside the prototype's LH-TES. To account for the effect of subcooler in the HTHP performance an additional constant subcooling value was set at 61 K (this value was selected based on EES-CHEST model results). Table 3 summarizes the results of this study.

Table 3. Parametric study for the preliminary HTHP model

Component	$T_{source,CHEST}=T_{source,HTHP}$ [°C]→	40	55	70	85*	100
Compressor	Total Power [kW]	4.15	6.11	8.15	10.74	13.52
	Ref. mass flow rate [kg/s]	0.037	0.091	0.167	0.27	0.416
	Pressure ratio (Pr) [-]	11.5	7.41	4.98	3.51	2.51
Condenser	Capacity [kW]	5.24	10.49	18.42	30	47.1
	T_{cond} [°C]	134	134.58	135.09	135.75	136.58
Evaporator	Capacity [kW]	5.35	13.78	26.85	45.49	73.51
	T_{evap} [°C]	34.1	48.36	62.62	76.61	91.27
HTHP Performance	Total heat stored [kW] (condenser+subcooler)	9.52	19.98	34.52	54.59	83.63
	COP_{HTHP} [-]	2.3	3.27	4.23	5.08	6.18

* The highlighted column represents the results for the nominal point of CHEST system prototype.

It can be noticed in the case of $T_{source,CHEST}=40$ °C, the Pr value reached 11.5 with low COP value of 2.3, so this case was excluded from further simulation studies.

3.3. HTHP Components selection and design

The previous preliminary results give us a general idea about the overall system performance and HTHP limits. Based on this, the EES-CHEST model, refer to Section 2.3 for more details about the model and assumptions, 2.3 was updated. To select the different components of the CHEST system prototype, the EES-CHEST model was used for source temperature= 100 °C, while the sink temperature was fixed at 25 °C. These limits were selected to give the maximum capacity and mass flow rates for the heat exchangers. The inputs to the model are summarized in the following points:

- The pinch point approach in heat exchangers is set to 5 Kelvin.

- The water-side temperature lift in both HTHP's evaporator and ORC's condenser was fixed to 5 K.
- SH value of 5 K is fixed inside the HTHP's evaporator and ORC's LH-TES.
- The pressure drops inside heat exchangers is neglected.
- The HTHP's compressor overall and volumetric efficiencies are constant and equal, respectively, to 0.6 and 0.7.
- The HTHP's compressor has 1 cylinder with swept volume of 515 cm³, and works under fixed speed of 1500 rpm.
- The ORC's expander isentropic, mechanical, and electrical efficiencies are set to: 0.7, 0.99, and 0.98, respectively.
- The ORC's main pump isentropic, mechanical, and electrical efficiencies are set to: 0.7, 0.99, 0.95, respectively.

3.3.1. Condenser

Based on EES-CHEST model prediction, Figure 18 shows the temperature profiles inside the HTHP's condenser.

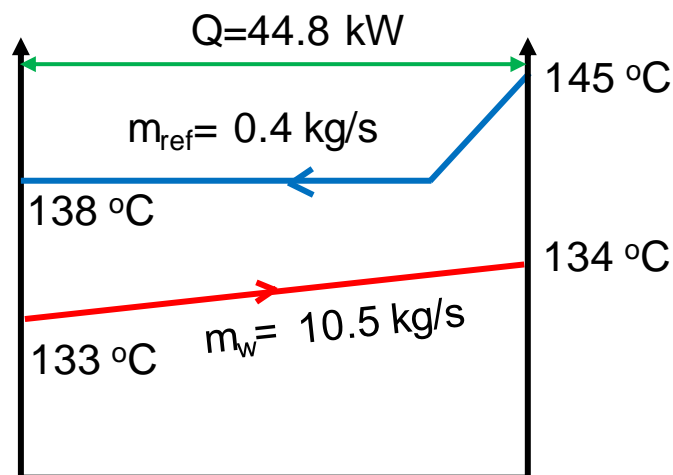


Figure 18. Temperature profiles inside HTHP's condenser for $T_{\text{source,CHEST}} = 100$, $T_{\text{melt,PCM}} = 133$, and $T_{\text{sink,CHEST}} = 25 \text{ }^\circ\text{C}$.

These results were used in SWEP selection tool (SSP G8) [15] to select the proper condenser. The SSP G8 recommended utilizing B200TH condenser with number of plates= 106, heat transfer area= 13.4 m², width= 243 mm, height= 525 mm, and depth= 253 mm.

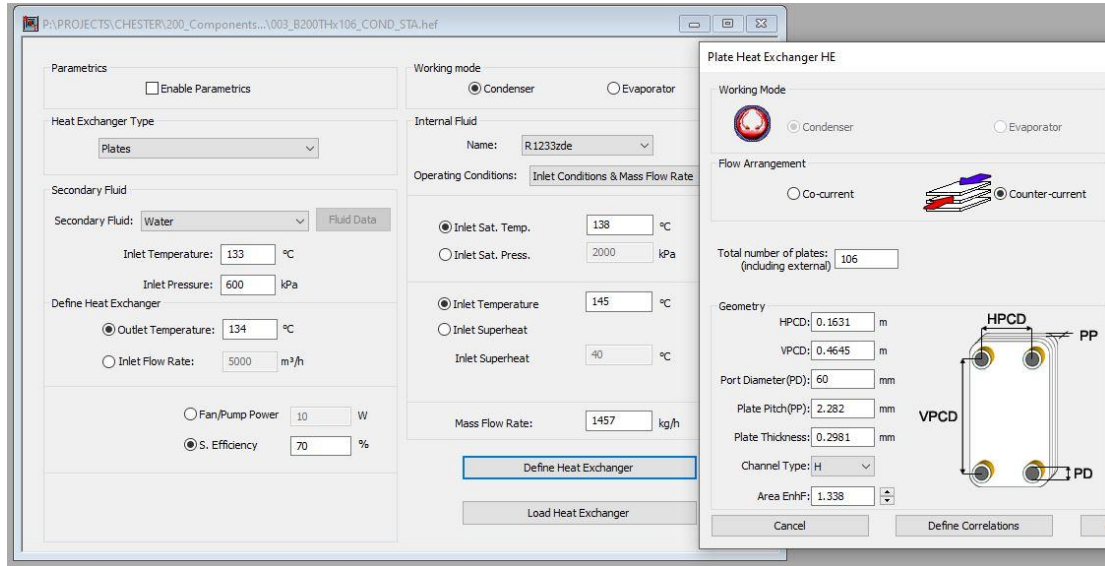


Figure 19. SWEP B200TH condenser model in IMST-ART®.

This condenser was modeled in IMST-ART as a stand-alone heat exchanger (Figure 19) to validate its performance with the manufacturer’s catalog data.

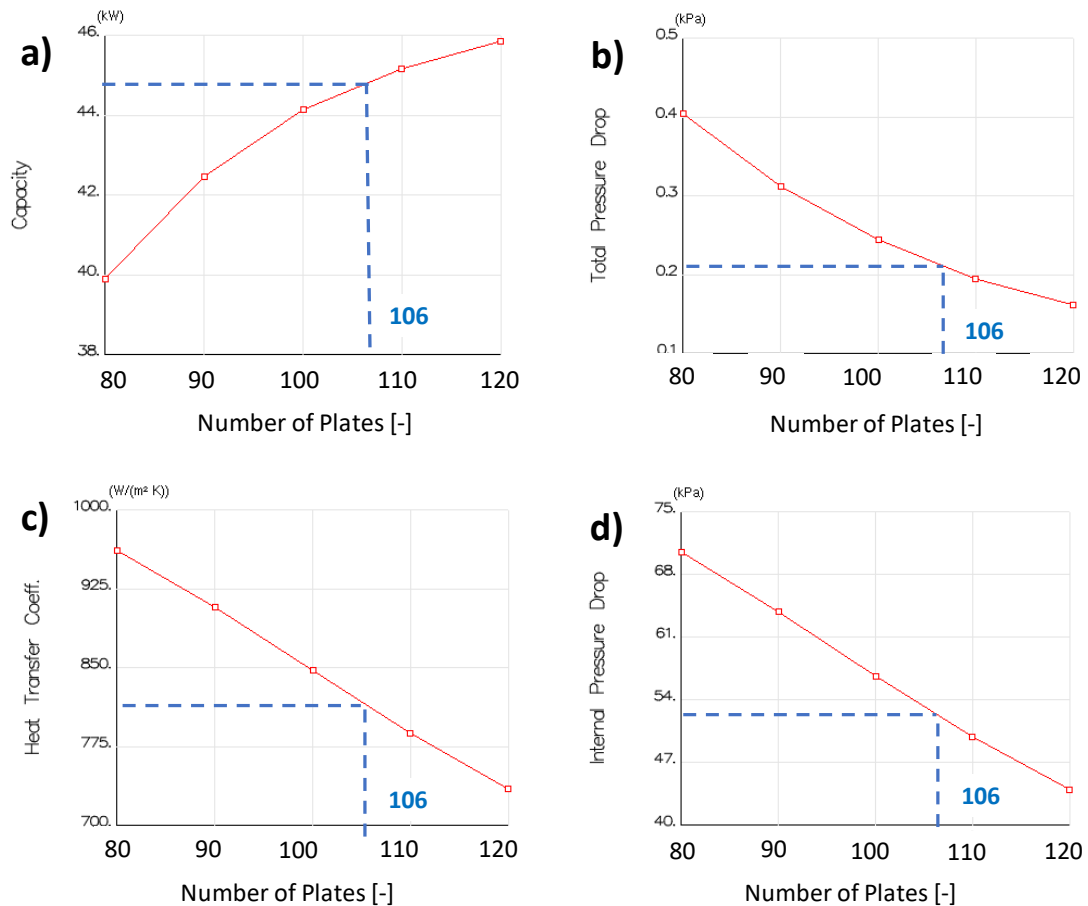


Figure 20. Effect of number of plates on SWEP B200TH condenser performance: a) Thermal capacity, b) refrigerant-side pressure drop, c) refrigerant-side HTC, and d) water-side pressure drop.

Figure 20 shows the effect of changing the number of plates (NoPs) on the condenser capacity, refrigerant-side pressure drop, refrigerant-side heat transfer coefficient (HTC), and water-side

pressure drop. In this study the inlet and outlet temperatures of water were fixed at 133 and 134 °C, respectively. Regarding the refrigerant-side, the inlet temperature and mass flow rate were set to 145 °C and 0.4 kg/s, respectively. It can be seen that increasing the NoPs by 20% (from 100 to 120) results to an increase in the condenser's capacity by only 3.9% (Figure 20a) and a decrease in the refrigerant-side pressure drop by 33.8% (Figure 20b). But, generally, the refrigerant-side pressure drop is very small and does not exceed 0.5 kPa. Also, it can be seen in Figure 20c that the refrigerant-side HTC ranges between 962 W/m².K (for NoPs= 80) to 735 W/m².K (for NoPs= 120).

3.3.2. Subcooler

Based on EES-CHEST model prediction, for $T_{source,CHEST}=100$ °C, $T_{melt,PCM}=133$ °C, and $T_{sink,CHEST}=25$ °C, Figure 21 shows the temperature profiles inside the HTHP's subcooler.

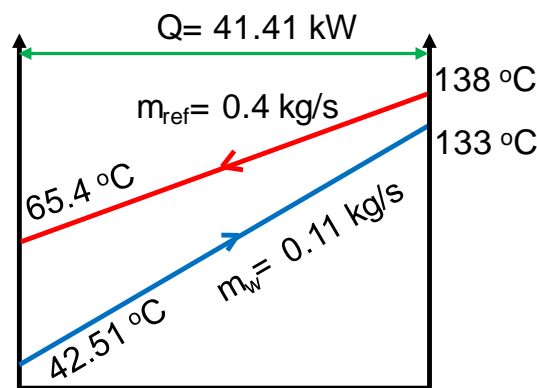


Figure 21. Temperature profiles inside HTHP's subcooler for $T_{source,CHEST}=100$, $T_{melt,PCM}=133$, and $T_{sink,CHEST}=25$ °C.

Regarding these results, SSP G8 recommended B86H single-phase heat exchanger with number of plates of 62, heat transfer area of 3.6 m², width of 119 mm, height of 526 mm, and depth of 108 mm. It should be mentioned that an over-surfacing (OS) value of 10% was adopted in order to reduce the pressure drop.

3.3.3. Evaporator

The HTHP's evaporator was selected in a similar way as the selection of condenser. Figure 22 shows the evaporator's temperature profiles predicted by the EES-CHEST model.

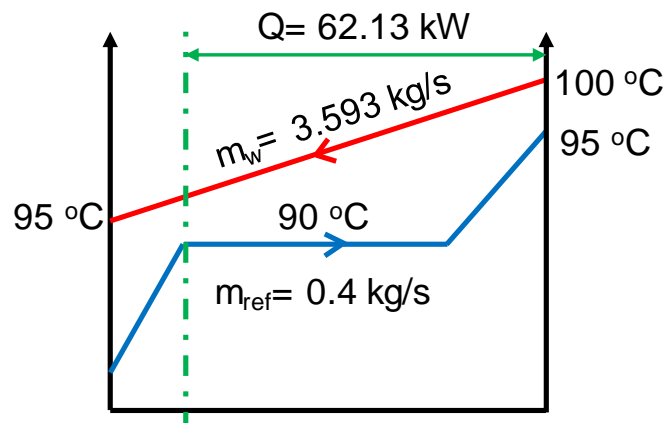


Figure 22. Temperature profiles inside HTHP's evaporator for $T_{source,CHEST}=100$, $T_{melt,PCM}=133$, and $T_{sink,CHEST}=25$ °C.

The recommended evaporator by SWEP's selection software for this capacity is V120TH with number of plates 60, heat transfer area of 7.66 m², width of 243 mm, height of 525 mm, and depth of 148 mm. An OS value of 72% was used to account for the subcooling portion of the evaporator and to coincide with the estimations of EES-CHEST model.

This evaporator was modeled using stand-alone heat exchanger feature inside IMST-ART[®] and was validated successfully with the catalog data. After the validation, the effect of changing the NoPs on the evaporator's performance was evaluated, as seen in Figure 23. In this parametric study the inlet and outlet water temperatures were kept constant at 100 and 95 °C, respectively. The SH value and refrigerant mass flow rate were set to 5 K and 0.4 kg/s, respectively. The inlet temperature of refrigerant is defined based on $T_{\text{cond}}=137.8$ °C and subcooling value of 71.1 °C.

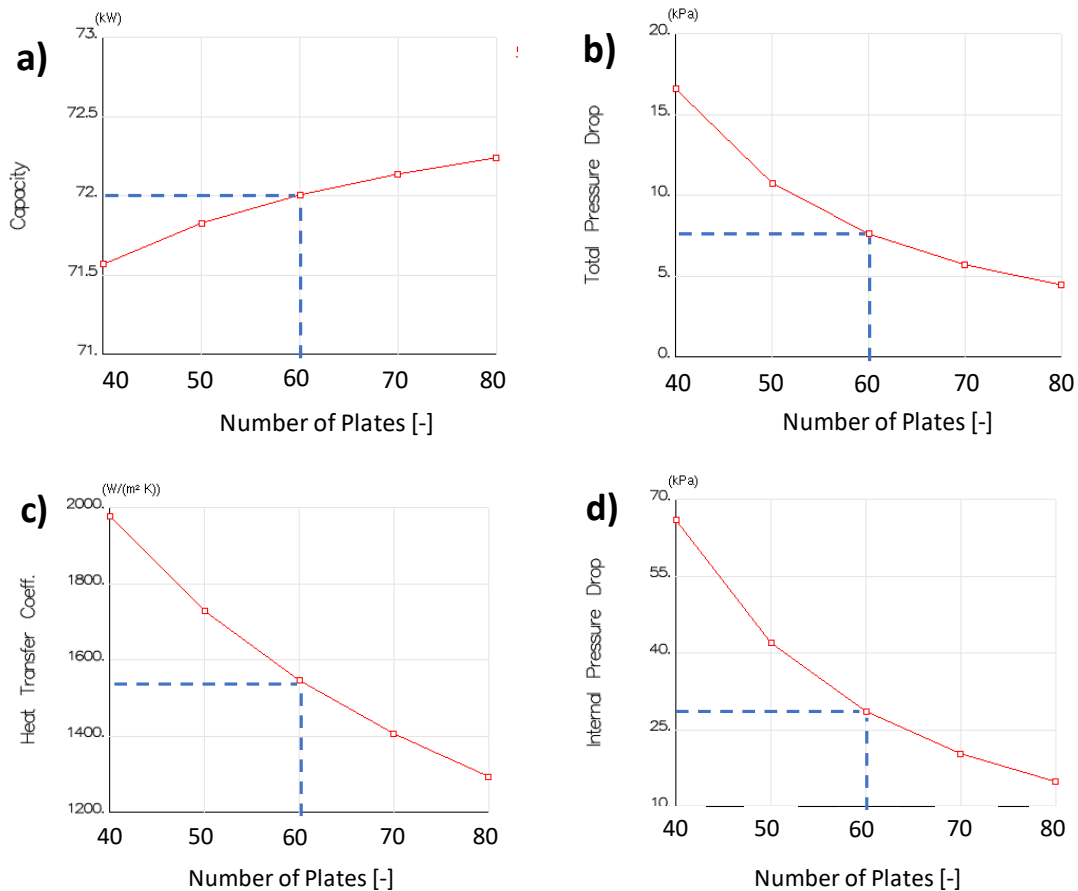


Figure 23. Effect of number of plates on SWEP V120TH evaporator performance: a) Thermal capacity, b) refrigerant-side pressure drop, c) refrigerant-side HTC, and d) water-side pressure drop.

It can be seen in Figure 23a that increasing the NoPs by 34% (from 60 to 80) the evaporator's capacity increases only by 0.32%. Figure 23b shows that the refrigerant-side pressure drop decreases by 41.4% with increasing the NoPs from 60 to 80. However, it can be seen that the maximum value is 16.6 kPa for NoPs= 40. The refrigerant-side HTC is shown in Figure 23c, it can be seen that it ranges between 1977 W/m²·K (for NoPs= 40) and decrease to 1295 W/m²·K (for NoPs= 80).

3.3.4. Expansion valve

The HTHP prototype will operate at higher temperatures than most of conventional HVAC systems. The range of operating temperature for the expansion devices is normally up to 75°C.

Moreover, expansion devices operate with a specific range of refrigerants which are normally the conventional fluids used in the refrigeration sector. R1233zdE is an alternative fluid which is not considered in most of the selection lists of the manufacturers. Since it is a prototype the control of the expansion device must be flexible and adjustable to a wide range of operating conditions. Therefore, the expansion valve must be capable to operate via a controlling algorithm which can only be done by the electronically controlled valves.

Therefore, the main points to consider for the selection of the expansion valve are:

- Very high operation temperature (up to 140°C)
- Capable to work with R1233zdE
- To be controlled electronically

After the study of the available electronic expansion valves (EEV) available in the market and the suggestions provided by the compressor manufacturer an EEV from SIEMENS has been selected. The selected EEV type is the MVL661 which is controlled with either 0-10V or 4-20mA signals. It is suitable to operate with HFO fluids and temperatures up to 140°C. The maximum operating pressure is 45 bar and the maximum differential pressure is 25bar. It has an accuracy during operation of 3% of full scale and its positioning time is 1sec. It also has two selectable operating ranges from 0-100% and 0-63% of its opening degree.

Type reference	DN	k_{ve} [m ³ /h]	k_{ve} reduced ¹⁾ [m ³ /h]	Δp_{max} [MPa]	$Q_2 E$ [kW]	$Q_2 H$ [kW]	$Q_2 D$ [kW]
MVL661.15-0.4	15	0.40		2.5	47	9.2	1.7
			0.25		29	5.7	1.0
MVL661.15-1.0	15	1.0			117	23	4.2
			0.63		74	14	2.6
MVL661.20-2.5	20	2.5			293	57	10
			1.6		187	37	6.6
MVL661.25-6.3	25	6.3		737	144	26	
			4	468	92	17	
MVL661.32-10	32	10		1.6	1170	230	42
			6.3		740	140	26
MVL661.32-12	32	12		0.2	*)	*)	50
			8		*)	*)	33

¹⁾ 63% of k_{ve} , refer to "k_{ve} reduction" on page 4
²⁾ MVL661.32-12.0 is only approved for suction throttle applications
 k_{ve} Nominal flow rate of refrigerant through the fully open valve (H_{100}) at a differential pressure of 100 kPa (1 bar) to VDI 2173
 $Q_2 E$ Refrigeration capacity in expansion applications
 $Q_2 H$ Refrigeration capacity in hot-gas bypass applications
 $Q_2 D$ Refrigeration capacity in suction throttle applications and $\Delta p = 0.5$ bar
 Q_2 With R407C at $t_2 = 0$ °C, $t_c = 40$ °C



Figure 24: Table for selection of the Electronic Expansion Valve.

The table of Figure 24 provided by the manufacturer determines a selection criteria according to the flow coefficient kv, which is considered as the maximum flow rate that can flow in fully open position with a differential pressure of 1bar. For the operating temperatures of 60°C evaporating and 138°C condensing the pressure difference across the EEV is calculated 18,2 bar. The maximum volumetric flow rate is calculated for the models MVL661.15-0.4 and MVL661.15-1.0 considering both operating ranges 100% and 63%.

Table 4. Results from the selection procedure of the MVL661 electronic expansion valve.

Operating conditions EEV					
Pressure evap. (@60°C)	bar-a	3,91			
Pressure cond. (@138°C)	bar-a	22,11			
Temp. SubC outlet	°C	70			
Max. mass flow rate	kg/s	0,385			
Density of fluid	kg/m ³	1144,5			
Differential pressure	bar	18,2			
		MVL661.15-0.4		MVL661.15-1.0	
Flow coef. SIEMENS (k _v)	m ³ /h	0,4	0,25	1	0,63
EEV max. vol. flow rate	m ³ /h	1,60	1,00	3,99	2,51
EEV max. mass flow rate	kg/s	0,51	0,32	1,27	0,80
Opening degree		76%	121%	30%	48%

According to the calculations based on a refrigerant flow rate of 0,385kg/s and 70°C fluid temperature, the MVL661.15-1.0 is the best suitable expansion device as presented in Table 4. Under partial operation of 63% the opening degree of the expansion valve is at 48%.

3.3.5. Refrigerant lines

The diameter of suction, discharge, and liquid lines were estimated by the IMST-ART[®] to ensure low pressure drop while maintain an adequate refrigerant velocity. Table 5 and Table 6 shows the refrigerant lines specifications, refrigerant velocity and pressure drop values for compressor speeds of 500 and 1500 rpm, respectively.

Table 5. Refrigerant lines specifications for compressor speed of 500 rpm.

Component	T _{source,CHEST} =T _{source,HTHP} [°C]	100	85	70	55
Discharge Line	External diameter	28.6	28.6	28.6	28.6
	[mm(inch)]	(1 1/8")	(1 1/8")	(1 1/8")	(1 1/8")
	Internal diameter [mm]	26.06	26.06	26.06	26.06
	Length [m]	2	2	2	2
	Insulation thickness [mm]	20	20	20	20
	Refrigerant velocity [m/s]	2.1353	1.3574	0.82372	0.45434
	Total pressure drop [kPa]	1.5727	1.103	0.8832	0.75387
	Heat loss [W]	49.657	48.255	47.12	47.714
Liquid Line	External diameter	34.90	34.90	34.90	34.90
	[mm(inch)]	(1 3/8")	(1 3/8")	(1 3/8")	(1 3/8")
	Internal diameter [mm]	32.1	32.1	32.1	32.1
	Length [m]	0.5	0.5	0.5	0.5
	Insulation thickness [mm]	none	none	none	none
	Refrigerant velocity [m/s]	0.16992	0.10941	0.067134	0.036011
	Total pressure drop [kPa]	1.3667	1.3462	1.3379	1.3343
	Suction Line	External diameter	34.90	34.90	34.90
[mm(inch)]		(1 3/8")	(1 3/8")	(1 3/8")	(1 3/8")
Internal diameter [mm]		32.1	32.1	32.1	32.1
Length [m]		2	2	2	2
Insulation thickness [mm]		20	20	20	20
Refrigerant velocity [m/s]		3.8584	3.5584	3.1338	2.4867
Oil drag min. velocity [m/s]		1.6716	2.0015	2.4006	2.9279
Total pressure drop [kPa]		0.52892	0.31995	0.16501	0.049141
Heat loss [W]	33.89	26.468	19.479	12.5	

It can be noticed that for very low compressor speed (500 rpm) and low source temperature (55 °C) the actual refrigerant velocity in the suction line is a little bit less than the required minimum oil drag velocity, however we expect not to face this situation to much in the CHEST prototype system.

Table 6. Refrigerant lines specifications for compressor speed of 1500 rpm.

Component	T _{source,CHEST} =T _{source,HTHP} [°C]	100	85	70	55
Discharge Line	External diameter	28.6	28.6	28.6	28.6
	[mm(inch)]	(1 1/8")	(1 1/8")	(1 1/8")	(1 1/8")
	Internal diameter [mm]	26.06	26.06	26.06	26.06
	Length [m]	2	2	2	2
	Insulation thickness [mm]	20	20	20	20
	Refrigerant velocity [m/s]	5.5761	3.6071	2.23	1.2524
	Total pressure drop [kPa]	5.8847	3.06	1.7011	1.0253
	Heat loss [W]	50.545	49.021	48.027	49.265
Liquid Line	External diameter	34.90	34.90	34.90	34.90
	[mm(inch)]	(1 3/8")	(1 3/8")	(1 3/8")	(1 3/8")
	Internal diameter [mm]	32.1	32.1	32.1	32.1
	Length [m]	0.5	0.5	0.5	0.5
	Insulation thickness [mm]	none	none	none	none
	Refrigerant velocity [m/s]	0.46425	0.30004	0.18459	0.098252
	Total pressure drop [kPa]	1.5885	1.443	1.3747	1.3427
	Suction Line	External diameter	34.90	34.90	34.90
[mm(inch)]		(1 3/8")	(1 3/8")	(1 3/8")	(1 3/8")
Internal diameter [mm]		32.1	32.1	32.1	32.1
Length [m]		2	2	2	2
Insulation thickness [mm]		20	20	20	20
Refrigerant velocity [m/s]		11.288	10.367	9.078	7.1225
Oil drag min. velocity [m/s]		1.7325	2.0645	2.463	2.9909
Total pressure drop [kPa]		5.3282	3.3666	1.9383	0.87191
Heat loss [W]	32.722	25.598	18.894	12.127	

3.3.6. Accessories

The compressor is operating with a fluid not tested by the manufacturer and the testing conditions could be out of the operational conditions of both the compressor and the testing rig. Considering also the importance of the compressor, a few auxiliary components were installed.

Suction accumulator

The suction line must be equipped with a suction accumulator to prevent liquid refrigerant entering the compressor. If liquid droplets enter the compressor's cylinder the piston and internal parts of the compressor can be damaged. In addition, the suction accumulator helps the oil flow back to the compressor via a hole that is drilled in the bottom of the internal U-tube.

The selected accumulator is the LCY 1011 from CARLY, with a volume capacity of 9.4 l. Both the inlet and outlet connections have an OD of 1-3/8". According to the manufacturer the maximum temperature and pressure of the accumulator are 120 °C and 20 bar respectively.



CARLY references		Drawing Nb	Dimensions (mm)				Possible retention volume (L)	Net weight (kg)
			Ø1	L	E1	Ø2		
LCY 04 S	LCY 04 MMS	1	89,0	208,0	50	/	0,09	1,20
LCY 14 S	LCY 14 MMS	1	89,0	299,0	50	/	0,09	1,70
LCY 15 S/MMS		1	89,0	299,0	48	/	0,10	1,80
LCY 16 S	LCY 16 MMS	1	89,0	299,0	37	/	0,12	1,95
LCY 25 S/MMS		1	101,6	363,0	56	/	0,13	3,15
LCY 26 S	LCY 26 MMS	1	101,6	363,0	56	/	0,12	3,20
LCY 27 S	LCY 27 MMS	1	101,6	373,0	56	/	0,14	3,30
LCY 47 S	LCY 47 MMS	1	101,6	487,0	56	/	0,14	4,35
LCY 49 S	LCY 49 MMS	2	121,0	464,5	49	/	0,16	5,60
LCY 69 S	LCY 69 MMS	2	152,4	433,5	76	/	0,21	8,20
LCY 89 S	LCY 89 MMS	2	152,4	533,5	76	/	0,21	8,85
LCY 811 S/MMS		2	152,4	439,0	76	/	0,25	9,10
LCY 811 S/MMS		2	152,4	539,0	76	/	0,25	11,20
LCY 813 S	LCY 813 MMS	2	152,4	539,0	73	/	0,25	11,60
LCY 1011 S/MMS		2	152,4	647,0	76	/	0,25	13,65

Figure 25: Diagram of CARLY suction accumulator and table of dimensions.

Things to consider:

- The capacity of the selected accumulator in kg of refrigerant must be higher than 50% of the installation’s total refrigerant load.
- Mounting should be exclusively performed in vertical position, as close as possible to the compressor and at the same height.
- For optimal operation, the refrigerant flow speed in the suction line accumulator’s rods should be between 8 and 12 m/s; for lower speed values, the oil return to the compressor is unsure.

Oil separators

Considering the long distance and the height difference that the mixture oil/refrigerant must travel in the entire pipeline of the cycle, an oil separator must be installed. The oil separator will be installed at the discharge line. It is equipped with a helical oil separator to force the oil to separate via centrifugal forces. The oil is collected at the bottom of the separator and a valve-float-needle system allows the oil to exit the separator. The oil outlet is connected via a pipeline to the suction line right after the suction line separator. According to the manufacturer it is possible to connect the oil return pipe directly to the compressor crankcase, but the VHE compressor is not equipped with a port for this function.

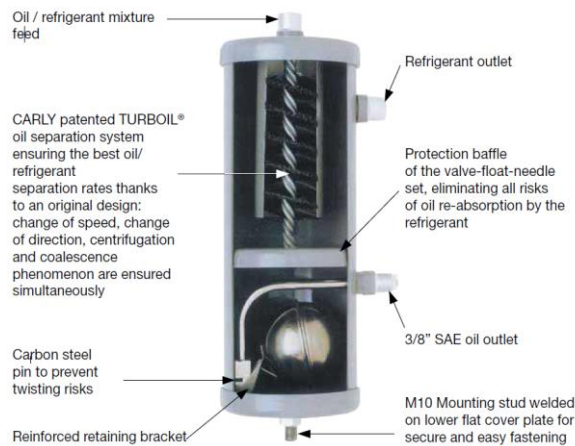


Figure 26: Diagram showing the internal parts of the TURBOIL discharge line separators.

The selected oil separator is the Turboil 3009 S made by CARLY which is compatible with HFO fluids. Its internal volume is 2.54 l and the oil storage volume is 0.3 l. The maximum operation temperature and pressure are 140°C and 46 bar respectively. The refrigerant inlet and outlet connections have an OD of 1-1/8" and the oil outlet connection has an OD of 3/8".

To consider:

- It must be thermally insulated to avoid any type of refrigerant condensation
- The oil separation performance depends directly on the flow rate of the mixture oil/refrigerant
- It must be installed vertically on the discharge line as close as possible to the compressor.
- The efficiency of the separation is 99%, therefore, additional oil level monitoring must be performed during the HTHP operation.

CARLY references				Dimensions mm						
		Connections types (1)	Drawing No	Ø1	Ø2	L	E1	E2	E3	E4
TURBOIL 1503 S	TURBOIL 1503 MMS	2	1	101,6	109,0	283	80	71	175	84
TURBOIL 1504 S	TURBOIL 1504 MMS	2	1	101,6	109,0	283	80	71	175	84
TURBOIL 2505 S/MMS		2	1	101,6	109,0	305	82	73	197	84
TURBOIL 3006 S	TURBOIL 3006 MMS	2	1	101,6	109,0	308	85	76	200	84
TURBOIL 3007 S/MMS		2	1	101,6	109,0	358	97	83	250	84
TURBOIL 3009 S	TURBOIL 3009 MMS	3	1	101,6	109,0	390	107	80	282	84



Figure 27: Diagram of CARLY oil separators and table with dimensions.

Liquid receiver

A liquid receiver is necessary in order to ensure the compensation of the refrigerant during volume variations caused by operating temperature or compressor speed changes. Moreover, during breakdown service or maintenance the liquid receiver works as refrigerant storage tank.

It must be mounted after the condenser and in a lower height than the condenser to avoid back-flow of the liquid during off-cycle periods.

The selected liquid receiver is the horizontal configuration RLHCY 400 made by CARLY. Its internal volume capacity is 40 liters and it is suitable to operate with HFO fluids. Its maximum operating temperature and pressure are 130°C and 45 bar respectively.

To consider:

- Liquid receivers are to be mounted after the condenser
- For optimal operation, special attention should be paid to the receivers' level: RLHCY receivers should be perfectly horizontal and RLVCY should be perfectly vertical.
- Liquid receivers ensure the compensation of refrigerant volume variations in refrigerating and air conditioning installations.
- These volume variations are due to fluctuations generated by various operating temperatures at various seasons, and to the opening and closing sequences of the expansion valve, which fills - or not - the evaporator with its refrigerant.

- Liquid receivers also allow storage of the whole installation’s refrigerant, for maintenance or breakdown service.

CARLY references	Outside of connections to screw UNF inch	Inside of connections to solder inch	Drawing No	Dimensions mm										
				Ø1	Ø2	L1	L2	E1	E2	E2	Ø3	L3	Ø4 NPTF inch	
RLNCY 15	3/4	1/4	1	88,9	95	343	298	210	44	/	/	M10	17,0	/
RLNCY 25	3/4	3/8	1	121,0	128	332	287	150	68	/	/	M10	17,0	/
RLNCY 30	3/4	3/8	1	121,0	128	368	323	186	68	/	/	M10	17,0	/
RLNCY 45	3/4	3/8	2	152,4	156	376	304	145	80	/	/	2 x Ø 10,5 x 9,5	17,0	/
RLNCY 60	1	1/2	2	152,4	156	459	387	228	80	/	/	2 x Ø 10,5 x 9,5	17,0	/
RLNCY 75	1	1/2	2	152,4	156	557	485	328	79	/	/	2 x Ø 10,5 x 9,5	17,0	/
RLNCY 90	1	1/2	3	152,4	156	258	595	436	80	192	/	4 x Ø 10,5 x 9,5	17,0	3/8
RLNCY 120	1 1/4	5/8	3	152,4	156	389	726	567	82	192	/	4 x Ø 10,5 x 9,5	22,5	3/8
RLNCY 150	1 1/4	3/4	3	168,3	172	352	746	582	82	200	/	4 x Ø 10,5 x 9,5	22,5	3/8
RLNCY 200	1 1/4	3/4	3	168,3	172	600	994	830	82	200	/	4 x Ø 10,5 x 9,5	22,5	3/8
RLNCY 250	1 1/4	3/4	3	168,3	172	750	1242	1078	109	200	/	4 x Ø 10,5 x 9,5	22,5	3/8
RLNCY 300	1 1/4	3/4	3	219,1	224	402	909	691	112	220	/	4 x Ø 10,5 x 9,5	22,5	3/8
RLNCY 400	1 3/4	1 1/8	3	219,1	224	690	1202	979	112	220	/	4 x Ø 10,5 x 9,5	22,5	1/2

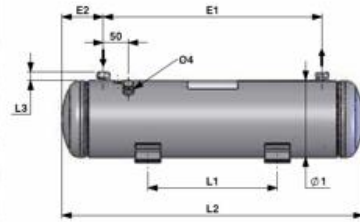


Figure 28: Table with the dimensions of the Carly liquid receiver and diagram.

Filter drier

A filter/drier will be mounted to maintain moisture, acid and impurities away of the system. In addition, it protects the expansion device from metallic debris. It will be installed on the liquid line after the liquid receiver and upstream the expansion element. The selected filter is the BCY-HP 489 made by CARLY, it is a Platinum filter with exchangeable cores. It is suitable for HFO fluids and its maximum operating temperature and pressure are 140°C and 46 bar respectively. Its filtering fineness is 150 microns with filtering surface of 420 cm².

Things to consider:

- Careful selection of the solenoid valves located downstream of the filter drier shells; their oversizing could cause liquid hammer phenomena hindering the filter drier shells’ proper mechanical behavior;
- Do not install the filter drier in an area of the circuit that can be isolated.

CARLY references	Connection types (1)	Filtering surface cm ²	Dimensions mm							
			Ø1	Ø2 (2)	Ø3	L1	L2	E1	E2	
BCY-HP 485 S/MMS	2	420	121	128	150	223	210	139	83	
BCY-HP 487 S/MMS	2	420	121	128	150	233	210	149	93	
BCY-HP 489 S	BCY-HP 489 MMS	3	420	121	128	150	238	210	154	98
BCY-HP 4811 S/MMS	3	420	121	128	150	247	210	163	108	

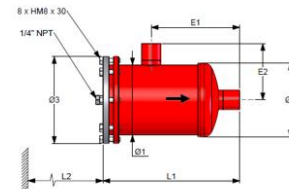


Figure 29: Table of dimensions of the selected filter drier.

Sight glasses

The state of the fluid within the refrigeration cycle can be determined based on the conditions measured. However, it is good practice to install sight glasses (SG) to provide a visual reference of the refrigerant in the liquid and the vapor lines. The SG at the liquid line will be positioned at the inlet of the expansion device to monitor the phase of the fluid which in this case must be 100% liquid. The SG at the vapor line will be positioned at the suction line to provide visual feedback that only fluid in vapor phase is entering the compressor. The selected SG are the Danfoss SGI model for 1-3/8” OD solder connections.

Table 7. Instrumentation and control system.

Type	Code	Name	Comments
Component	C140	Compressor	VHE compressor
	EH140A/B	Electrical heater A and B	2 x 1 kWe oil heaters
	W101	Evaporator	SWEP PHE evaporator
	W102	Condenser*	SWEP PHE condenser
	W103	Subcooler	SWEP PHE subcooler
	W104	Air-to-water HX	Variable speed fan-coil
	V102	Solenoid valve	Electric solenoid valve
	V101	Electronic expansion valve	Siemens EXV
	P140	Motor cooling pump	
	P150	Evaporator's water pump	
	P160	Subcooler's water pump	
	B101	Suction-line accumulator	
	B102	Oil separator	
	B103	Liquid Receiver	
	PLC	Programable logic controller	Beckhoff PLC
	Inverter	Compressor's inverter	Siemens Sinamics S120
	Instrumentation	TT	Temperature transmitter
TC		Temperature control loop	Implemented in the PLC
PT		Pressure transmitter	4 – 20 mA pressure sensors
PS		Pressure switch	Safety pressure switch
PI		Pressure indicator	Indicators
FT		Flow transmitter	flowmeters
FS		Flow switch	Connected to PLC
FC		Flow control loop	Implemented in the PLC

* The condenser is only required for tests of the HTHP independently from the whole CHEST prototype. Once integrated into the full CHEST system, the condensing process will take place inside the LH-TES.

According to Figure 30, the heat pump control system can be divided into the following control loops:

- Main control loop (refrigerant circuit control loop).
- Evaporator control loop.
- Subcooler control loop.
- Compressor's motor cooling control loop.
- Auxiliary control loops (oil heaters, suction-line heat tracing, etc.).

Each one of these control loops are explained into more detail in the following sections.

4.1.1. Main control loop

In general terms, the operation of the HTHP is based on achieving a constant refrigerant superheating degree at the inlet of the compressor. By monitoring the pressure and temperature of the refrigerant at the compressor's suction-line, the degree of superheating is continuously calculated. If the calculated superheating degree doesn't match the designated set-point for this variable (i.e.: 10 Kelvin), the electronic expansion valve will adapt its percentage of openness in order to meet the desired condition.

The control strategy considered for the main control loop is based on always operating with a fixed compressor speed. According to this, the condensing temperature will fluctuate to have enough temperature difference between the refrigerant and the PCM's phase-changing

temperature. When considering this control strategy, at the beginning of the PCM's charging process the temperature difference in between the refrigerant and the PCM material will be rather small, however it will gradually increase as the PCM within the LH-TES becomes fully melted. When this happens, the compressor discharge temperature will also gradually increase. If the maximum temperature limit is not reached, there is no need to modify anything else. If the temperature limit is reached, then either the heat pump is switched off or the compressor speed is decreased in order to keep the discharge temperature below the maximum allowed value.

When considering this operation strategy, the heat capacity transferred to the PCM will be quite constant since the compressor speed is constant, and the pressure increase will be moderate. If a higher temperature difference is desired, the system can be operated with a higher compressor speed.

4.1.2. Evaporator control loop

The main objective of this control loop is to provide a constant temperature difference across the water-side of the HTHP's evaporator. As a rule-of-thumb, 5 Kelvin of temperature difference can be defined as the desired set-point for this system. This provides a good compromise in between achieving a good (high) evaporating temperature in the refrigerant-side, without having a significant impact on the expected water-side pressure loss, thus minimizing the water pump power consumption.

The control of this system is achieved by means of controlling the evaporator's water-side flowrate. The inlet and outlet water-side temperatures are continuously recorded and therefore their temperature difference is calculated. If the calculated value is different from the desired set-point, the HTHP's control unit will act over the water pump speed in order to maintain the desired temperature difference in between the inlet and outlet ports.

In addition, in this system the measurement of the water flowrate is registered by a dedicated flowmeter, while a flow switch will be used as an extra security within the control algorithm in order to avoid the operation of the compressor if there is no water flow detected across the evaporator.

4.1.3. Subcooler control loop

The subcooler's control loop seeks to obtain the highest possible water-side outlet temperature in this system. By doing this, the SH-TES will receive the water to be accumulated in the hot water tank at the highest possible temperature, therefore maximizing the achievable CHEST system efficiency.

The HTHP's control unit will continuously regulate the subcooler's water-side flowrate in order to achieve a constant temperature difference in between the refrigerant's inlet temperature and the water-side outlet temperature (i.e.: 3 Kelvin). In this way, we can ensure that the water is provided to the SH-TES at a value very close to the maximum achievable temperature while not forcing the water-side flow to tend to zero.

This control loop also considers a water-side flowmeter, which will be used to monitor the operation of the subcooler as well for all calculations required in the evaluation of the whole system. On the other hand, this system doesn't consider a flow switch because the subcooler's

operation is independent from the compressor's operation (the HTHP can work even without the subcooler into operation, just as a regular heat pump only with the condensing part).

4.1.4. Compressor's motor cooling control loop

Another critical control loop is the one in charge of the cooling of the compressor's electrical motor. VHE compressor's motor is "encapsulated" within a water-cooled crankcase (water jacket), thus cooling of the electrical motor can be achieved by extracting heat into the cooling water circuit. The HTHP prototype will consider a closed water circuit for the cooling of the motor. This circuit will mainly consist on a water pump and an fan-cooler in order to dissipate the rejected heat to the ambient air.

The control of this cooling system will work as a thermostat control; a motor temperature set-point is defined (i.e.: 110°C). With the water pump operating at a constant speed, the HTHP's control unit will act over the fan speed in order to maintain the motor below the desired temperature.

4.1.5. Auxiliary control loops

Additional control loops are going to be implemented in the HTHP's control system. However, the most relevant auxiliary control loops are briefly described here after:

- **Oil heaters:** the compressor considered for the HTHP prototype has two independent oil heating elements (1 kW each). These electrical heaters are going to be controlled by the HTHP's control unit with the aim to always maintain a minimum oil temperature when the compressor is in the stand-by condition. They will work according to a thermostat control loop philosophy, considering two heating steps (1 kWe or 2 kWe).
- **Suction-line heat tracing:** the compressor's suction-line will consider a heat tracing system in order to provide a pre-heating of the pipes and components of the suction-line circuit. Pre-heating this circuit allows to achieve a better and smoother start-up of the heat pump because it minimizes problems related to liquid (or liquid droplets) entering the compressor's pistons. The control of this system will also work according to the thermostat philosophy.
- **Compressor start-up protection:** As a safety measure, the compressor should not start more than 8 times per hour, with no less than 2 minutes between each start.

4.2. Operation control

As mentioned in section 4.1.1, the main control loop for controlling the heat pump when working at its normal operation condition is mainly based on achieving a constant superheating degree at the compressor's suction-line.

The HTHP control algorithm used for this purpose is based on the "Antoine's equation" for temperature. This equation will allow the control system to continuously calculate the saturated temperature at the compressor's inlet condition.

$$T = \frac{A_0}{\log_{10}(P) - A_2} - A_1 \quad (1)$$

Where,

A_0 , A_1 and A_2 are the identified coefficients of Antoine's equation for R1233zd(E).

P is the absolute pressure at the compressor's suction-line.

When the saturated temperature is calculated, the suction-line setpoint temperature is obtained by the following equation:

$$T_{exv,sp} = T + \Delta T_{sh,sp} \quad (2)$$

Where

$\Delta T_{sh,sp}$ is the suction-line superheating temperature setpoint (desired superheating)

Then, we need to compare the calculated temperature with the measured temperature at the compressor's suction-line. If the two temperatures are different, the expansion valve PID-based control algorithm will act over the valve opening degree in order to meet the required condition (meet the desired superheating degree at the compressor's suction-line).

4.3. Start-up procedure

The start-up procedure of the HTHP will need to be adjusted during the experimental testing phase. However, in general terms, the main actions to accomplish for the system start-up are the following:

- First, the whole system should be switched into the ON condition. Thus, the HTHP will enter first into the "stand-by" status. In this condition, the following actions are considered:
 - The oil heating system is set to ON.
 - The suction-line heat tracing system is set to ON.
- When the START order is given, first the system will evaluate if the starting conditions are met. Therefore, the following conditions are checked:
 - If the oil temperature is above the minimum required temperature.
 - If the suction-line temperature is above the minimum required temperature.
 - If there are no alarms (including compressor's motor temperature).
 - And if the number of starts has not been exceeded (See Section 4.1.5), then
- The system is set to the STARTING procedure. Which mainly considers the following actions:
 - The oil heaters and the heat tracing system are switched off.
 - The motor cooling pump and the evaporator's water pump are set to START. During the starting procedure, they are operated at constant speed.
 - After some pre-defined time, and if no alarms from both water flow switches are detected, the solenoid valve is set to OPEN and the electronic expansion valve is activated (its PID-based control algorithm is activated).
 - Then, the compressor can be set to START. The compressor will be gradually started from a low rotational speed up to the nominal speed by considering a predefined "speed-up ramp". This will be determined experimentally.
- Once the pressures and temperatures of the refrigerant are reaching a steady state condition, the following actions are considered:
 - The evaporator's and the motor cooling pumps are changed into variable speed operation. Thus, their speed is going to be controlled according to their own control strategy (See Sections 4.1.2 and 4.1.4).

- The subcooler's water pump is activated, and it will be controlled according to the assigned control strategy for this sub-system (See Section 4.1.3).

4.4. Shut-down procedure

The HTHP's control unit will have a dedicated shut-down procedure, which will be activated or executed when one of the following situations are met:

- The HTHP's START/STOP variable is set to STOP. This could be done either directly in the electrical and control cabinet control panel, or from an external supervisory control system (i.e.: laboratory's control room SCADA).
- If an ALARM is triggered.
- If the emergency button is pushed., or
- If the HTHP condensing pressure (related to the condensing temperature) exceeds the pre-defined maximum pressure defined in order to control the operation of the heat pump.

If the shut-down procedure is activated, the following actions will take place:

- The subcooler's water pump will be gradually speed-down according to predefine ramp-down curve. Then, the pump will be set to the STOP condition.
- The compressor will be gradually speed-down according to predefine ramp-down curve up to the minimum operating speed defined for this procedure.
- Once the compressor speed reaches the minimum operating speed, the compressor will be stopped (set to STOP).
- With the compressor completely stopped, the solenoid valve will be set to the CLOSE condition.
- The electronic expansion valve will be taken to the full closed position, and then it will be deactivated.
- The evaporator's water pump will gradually speed-down according to predefine ramp-down curve. Then, the pump will be set to the STOP condition.
- The motor cooling system will be left to work for 5 to 10 minutes, or until the motor temperature reaches a minimum temperature before it is set to STOP.

Once all these conditions are met, the "stand-by" status will be activated again, therefore, the HTHP will activate both, the oil heating and the suction-line heat tracing systems.

5. HTHP Prototype Estimated Performance under Steady-state Conditions

In the current section the IMST-ART[®] software is utilized to assess the performance of the proposed HTHP prototype for different source temperatures, compressor speeds, inlet water temperatures for the HTHP's subcooler (this equals to the low-temperature water tank temperature).

5.1. Effects of source temperature and compressor speed on the HTHP's performance

In the current study the fixed parameters for the HTHP model were:

- Refrigerant= R-1233zd(E).
- The subcooling in the HTHP's condenser= 0.2 K.
- Inlet and outlet water temperatures from the HTHP's condenser= 133 and 134 °C, respectively. These values are considered in order to more or less emulate the expected behavior inside the LH-TES system.
- The SH inside HTHP's evaporator= 5 K.
- The temperature lift for the water-side of HTHP's evaporator= 5K.
- Inlet and outlet water temperatures for the HTHP's subcooler= 43.8 and 133 °C, respectively¹; and
- The refrigerant line specifications are the same as the ones reported in Table 5 and Table 6.

while, the compressor speed was varied from 500 to 1500 rpm and source temperature ($T_{\text{source,HTHP}}$) ranged from 100 to 55 °C.

Figure 31 shows the HTHP's cycle on a P-h diagram for different source temperatures. It can be noticed that the subcooling value decreases with the decrease of the heat source temperatures. We see that a value of 70.5 K is obtained for a $T_{\text{source,HTHP}} = 100$ °C and of 61.5 K for $T_{\text{source,HTHP}} = 100$ °C. In the case of $T_{\text{source,HTHP}} = 70$ °C (Figure 31c). In the case of $T_{\text{source,HTHP}} = 70$ °C, a compressor's discharge superheating value of only 1.8 K is observed, which could give an indication to increase the SH inside the evaporator to avoid crossing the saturation line during actual operation. The discharge temperature has an average value of 140 °C. The pressure ratio (Pr) values varies from 2.7 to 7.9.

¹ These temperatures were reported by our partners from DLR in the e-mail received on 13/06/2019 regarding the design parameters for the CHEST prototype.

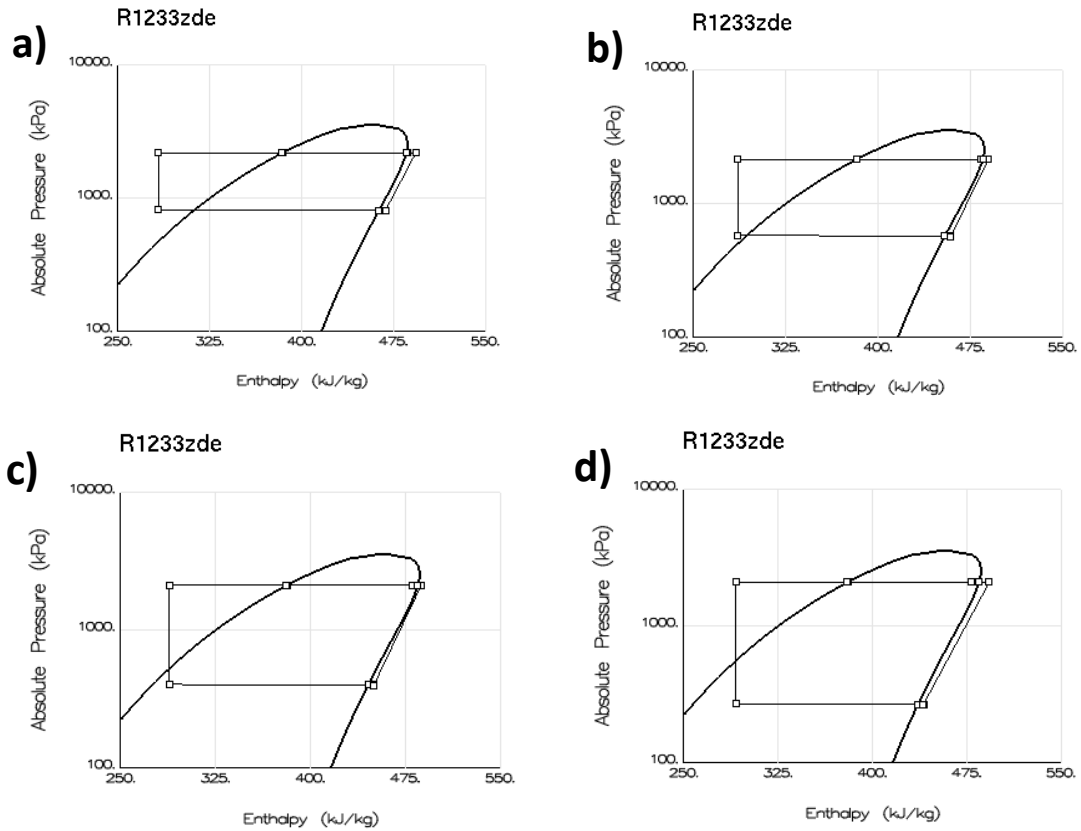


Figure 31. The HTHP's cycle on P-h diagram for compressor speed of 1500 rpm; and a) $T_{source,HTHP} = 100\text{ }^{\circ}\text{C}$, b) $T_{source,HTHP} = 85\text{ }^{\circ}\text{C}$, c) $T_{source,HTHP} = 70\text{ }^{\circ}\text{C}$, and $T_{source,HTHP} = 55\text{ }^{\circ}\text{C}$.

It can be seen in Figure 32 that the pinch point inside the HTHP's evaporator is always located at the beginning of the two-phase zone; it starts with a value of 6.4 K ($T_{source,HTHP} = 100\text{ }^{\circ}\text{C}$) and ends with a value of 3.1 K ($T_{source,HTHP} = 55\text{ }^{\circ}\text{C}$).

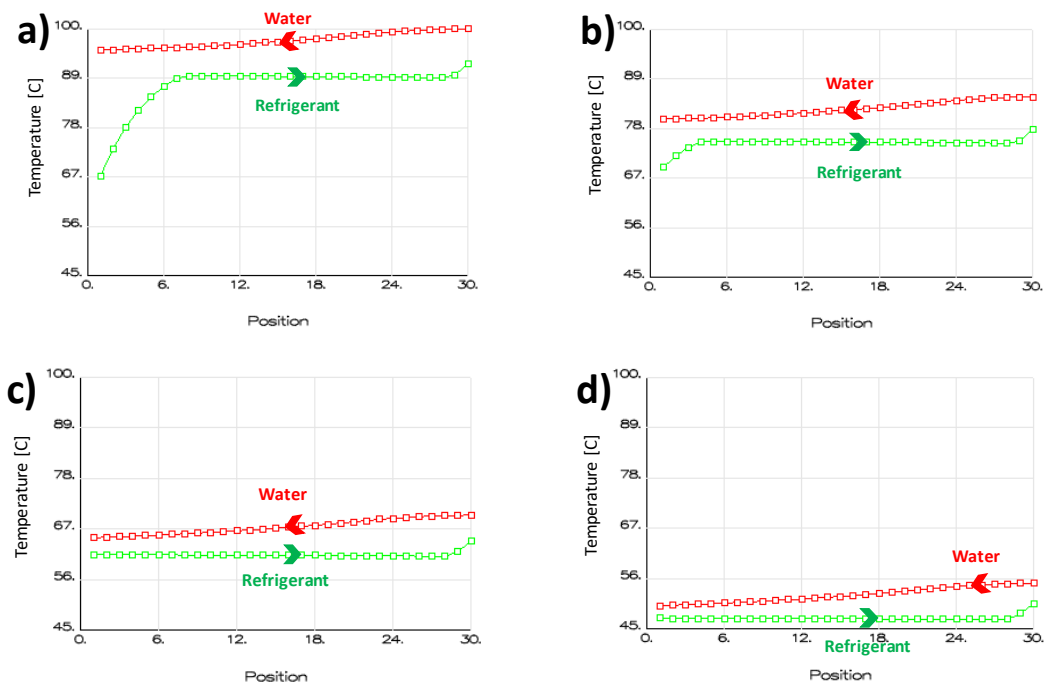


Figure 32. Temperature profiles inside HTHP's evaporator for compressor speed of 1500 rpm; and a) $T_{source,HTHP} = 100\text{ }^{\circ}\text{C}$, b) $T_{source,HTHP} = 85\text{ }^{\circ}\text{C}$, c) $T_{source,HTHP} = 70\text{ }^{\circ}\text{C}$, and $T_{source,HTHP} = 55\text{ }^{\circ}\text{C}$.

It can be seen (Figure 33) that the pinch point in the HTHP’s condenser is also located at the beginning of the two-phase zone. For $T_{source,HTHP} = 100\text{ }^{\circ}\text{C}$, the pinch point is 3.94 K, while it equals 1.43 K for $T_{source,HTHP} = 55\text{ }^{\circ}\text{C}$. In this case, the condensation temperature (bubble) starts with a value of 137.83 $^{\circ}\text{C}$ at $T_{source,HTHP} = 100\text{ }^{\circ}\text{C}$ and decreases to 135.36 $^{\circ}\text{C}$ at $T_{source,HTHP} = 55\text{ }^{\circ}\text{C}$.

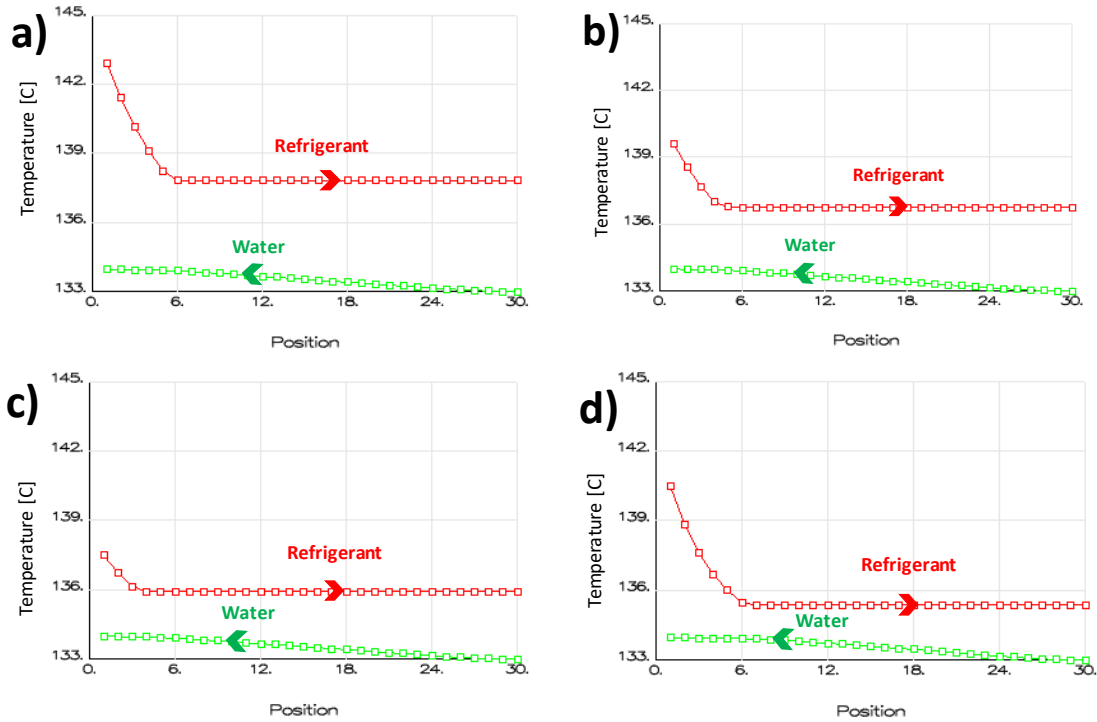


Figure 33. Temperature profiles inside HTHP’s condenser for compressor speed of 1500 rpm; and a) $T_{source,HTHP} = 100\text{ }^{\circ}\text{C}$, b) $T_{source,HTHP} = 85\text{ }^{\circ}\text{C}$, c) $T_{source,HTHP} = 70\text{ }^{\circ}\text{C}$, and d) $T_{source,HTHP} = 55\text{ }^{\circ}\text{C}$.

The detailed results for compressor speed of 500, 1000, and 1500 rpm are listed in Table 8, Table 9, and Table 10, respectively, for the given range of source temperatures.

Table 8. Effect of source temperature on the HTHP’s performance for compressor speed of 500 rpm, $T_{melt,PCM} = 133\text{ }^{\circ}\text{C}$, $T_{LTWT} = 43.8\text{ }^{\circ}\text{C}$, and $T_{HTWT} = 133\text{ }^{\circ}\text{C}$.

Component	$T_{source,CHEST} = T_{source,HTHP}\text{ }[^{\circ}\text{C}] \rightarrow$	100	85	70	55
Compressor	Total Power input [kW]	4.49	3.618	2.73	2.00
	Ref. mass flow rate [kg/s]	0.141	0.091	0.0554	0.0296
	Discharge temperature [$^{\circ}\text{C}$]	141.48	138.54	136.35	138.61
	Pressure ratio (Pr) [-]	2.46	3.46	4.957	7.429
Condenser	Capacity [kW]	15.711	9.858	5.917	3.255
	T_{cond} (bubble) [$^{\circ}\text{C}$]	136.01	135.4	134.89	134.59
	Ref-side pressure drop [kPa]	0.026	0.0061	0.0048	0.0085
Subcooler	Capacity [kW]	13.054	8.044	4.666	2.274
	Total subcooling [K]	64.631	61.808	58.359	52.932
	Ref-side pressure drop [kPa]	1.902	1.578	1.43	1.363
Evaporator	Capacity [kW]	25.582	15.345	8.662	4.131
	T_{evap} (dew) [$^{\circ}\text{C}$]	91.786	76.894	62.747	48.421
	Ref-side pressure drop [kPa]	1.342	0.9842	0.735	0.503
Global Performance	Total heat provided [kW] (condenser + subcooler)	28.765	17.902	10.583	5.529
	COP_{HTHP} [-]	6.406	4.95	3.877	2.765

Table 9. Effect of source temperature on the HTHP's performance for compressor speed of 1000 rpm, $T_{melt,PCM}=133\text{ }^{\circ}\text{C}$, $T_{LTWT}=43.8\text{ }^{\circ}\text{C}$, and $T_{HTWT}=133\text{ }^{\circ}\text{C}$.

Component	$T_{source,CHEST}=T_{source,HTHP}\text{ }[^{\circ}\text{C}]\rightarrow$	100	85	70	55
Compressor	Total Power input [kW]	8.898	7.086	5.35	3.948
	Ref. mass flow rate [kg/s]	0.268	0.173	0.106	0.0562
	Discharge temperature [$^{\circ}\text{C}$]	142.44	139.27	137.14	139.94
	Pressure ratio (Pr) [-]	2.603	3.634	5.154	7.678
Condenser	Capacity [kW]	29.489	18.636	11.292	6.275
	T_{cond} (bubble) [$^{\circ}\text{C}$]	137.06	136.18	135.47	135.02
	Ref-side pressure drop [kPa]	0.099	0.0415	0.0107	0.004
Subcooler	Capacity [kW]	26.174	16.171	9.478	4.794
	Total subcooling [K]	68.287	65.338	62.307	59.148
	Ref-side pressure drop [kPa]	3.295	2.176	1.664	1.432
Evaporator	Capacity [kW]	49.273	29.726	16.944	8.257
	T_{evap} (dew) [$^{\circ}\text{C}$]	90.267	75.647	61.778	47.608
	Ref-side pressure drop [kPa]	4.144	2.983	2.186	1.191
Global Performance	Total heat provided [kW] (condenser + subcooler)	55.663	34.807	20.77	11.069
	COP_{HTHP} [-]	6.256	4.912	3.882	2.804

Table 10. Effect of source temperature on the HTHP's performance for compressor speed of 1500 rpm, $T_{melt,PCM}=133\text{ }^{\circ}\text{C}$, $T_{LTWT}=43.8\text{ }^{\circ}\text{C}$, and $T_{HTWT}=133\text{ }^{\circ}\text{C}$.

Component	$T_{source,CHEST}=T_{source,HTHP}\text{ }[^{\circ}\text{C}]\rightarrow$	100	85	70	55
Compressor	Total Power input [kW]	13.21	10.433	7.891	5.860
	Ref. mass flow rate [kg/s]	0.385	0.249	0.153	0.0813
	Discharge temperature [$^{\circ}\text{C}$]	143.15	139.81	137.73	140.94
	Pressure ratio (Pr) [-]	2.726	3.776	5.318	7.865
Condenser	Capacity [kW]	41.977	26.663	16.274	9.134
	T_{cond} (bubble) [$^{\circ}\text{C}$]	137.83	136.76	135.92	135.36
	Ref-side pressure drop [kPa]	0.192	0.0872	0.0315	0.00364
Subcooler	Capacity [kW]	38.854	24.019	14.122	7.194
	Total subcooling [K]	70.496	67.376	64.344	61.539
	Ref-side pressure drop [kPa]	5.288	3.04	2.00	1.532
Evaporator	Capacity [kW]	71.306	43.171	24.722	12.126
	T_{evap} (dew) [$^{\circ}\text{C}$]	89.084	74.703	61.047	47.074
	Ref-side pressure drop [kPa]	7.924	5.664	4.103	2.17
Global Performance	Total heat provided [kW] (condenser + subcooler)	80.831	50.682	30.396	16.328
	COP_{HTHP} [-]	6.119	4.858	3.852	2.786

5.2. Effect of inlet water temperature to the subcooler (T_{LTWT}) on the HTHP's performance

In this study the inlet water temperature to the HTHP's subcooler ($T_{w,in,sc}$) was varied from 40 to 70 $^{\circ}\text{C}$. This temperature equals the low-temperature water tank's temperature. The nominal conditions was fixed in the current study, where $T_{source,HTHP}=85\text{ }^{\circ}\text{C}$, $\Delta T_{w,evap}=5\text{ K}$, and $T_{HTWT}=133\text{ }^{\circ}\text{C}$. Table 11, Table 12, and Table 13 show the results for compressor speeds of 500, 1000, and 1500 rpm, respectively.

Table 11. Effect of inlet water temperature to the subcooler on the HTHP's performance for compressor speed of 500 rpm, $T_{source,HTHP}=85\text{ }^{\circ}\text{C}$, $T_{melt,PCM}=133\text{ }^{\circ}\text{C}$, and $T_{HTWT}=133\text{ }^{\circ}\text{C}$.

Component	$T_{w,in,sc}=T_{LTWT}\text{ }[^{\circ}\text{C}]\rightarrow$	40	50	60	70
Compressor	Total Power input [kW]	3.616	3.626	3.646	3.655
	Ref. mass flow rate [kg/s]	0.09	0.091	0.0919	0.0923
	Discharge temperature [$^{\circ}\text{C}$]	138.54	138.57	138.64	138.66
	Pressure ratio (Pr) [-]	3.4658	3.453	3.426	3.414
Condenser	Capacity [kW]	9.851	9.90	10.01	10.058
	T_{cond} (bubble) [$^{\circ}\text{C}$]	135.4	135.4	135.41	135.42
	Ref-side pressure drop [kPa]	0.0061	0.00622	0.0065	0.0067
Subcooler	Capacity [kW]	8.313	7.625	6.956	6.214
	Total subcooling [K]	64.15	57.995	51.832	45.576
	Ref-side pressure drop [kPa]	1.577	1.58	1.585	1.587
Evaporator	Capacity [kW]	15.61	14.963	14.388	13.69
	T_{evap} (dew) [$^{\circ}\text{C}$]	76.872	77.026	77.361	77.51
	Ref-side pressure drop [kPa]	0.961	1.057	1.1665	1.237
Global Performance	Total heat provided [kW] (condenser + subcooler)	18.164	17.525	16.966	16.272
	COP_{HTHP} [-]	5.02	4.833	4.653	4.452

Table 12. Effect of inlet water temperature to the subcooler on the HTHP's performance for compressor speed of 1000 rpm, $T_{source,HTHP}=85\text{ }^{\circ}\text{C}$, $T_{melt,PCM}=133\text{ }^{\circ}\text{C}$, and $T_{HTWT}=133\text{ }^{\circ}\text{C}$.

Component	$T_{w,in,sc}=T_{LTWT}\text{ }[^{\circ}\text{C}]\rightarrow$	40	50	60	70
Compressor	Total Power input [kW]	7.082	7.102	7.158	7.187
	Ref. mass flow rate [kg/s]	0.172	0.173	0.176	0.177
	Discharge temperature [$^{\circ}\text{C}$]	139.26	139.3	139.39	139.43
	Pressure ratio (Pr) [-]	3.6368	3.623	3.586	3.568
Condenser	Capacity [kW]	18.613	18.713	18.982	19.121
	T_{cond} (bubble) [$^{\circ}\text{C}$]	136.18	136.19	136.21	136.22
	Ref-side pressure drop [kPa]	0.0414	0.0418	0.0431	0.0438
Subcooler	Capacity [kW]	16.696	15.338	14.069	12.631
	Total subcooling [K]	67.774	61.363	54.949	48.427
	Ref-side pressure drop [kPa]	2.174	2.183	2.205	2.217
Evaporator	Capacity [kW]	30.232	28.959	27.918	26.599
	T_{evap} (dew) [$^{\circ}\text{C}$]	75.612	75.769	76.194	76.415
	Ref-side pressure drop [kPa]	2.919	3.1472	3.53	3.77
Global Performance	Total heat provided [kW] (condenser + subcooler)	35.31	34.051	33.051	31.752
	COP_{HTHP} [-]	4.986	4.795	4.617	4.418

Table 13. Effect of inlet water temperature to the subcooler on the HTHP's performance for compressor speed of 1500 rpm, $T_{source,HTHP} = 85$ °C, $T_{melt,PCM} = 133$ °C, and $T_{HTWT} = 133$ °C.

Component	$T_{w,in,sc} = T_{LTWT}$ [°C] →	40	50	60	70
Compressor	Total Power input [kW]	10.424	10.462	10.558	10.612
	Ref. mass flow rate [kg/s]	0.248	0.250	0.254	0.256
	Discharge temperature [°C]	139.8	139.84	139.94	140
	Pressure ratio (Pr) [-]	3.78	3.763	3.722	3.70
Condenser	Capacity [kW]	26.623	26.792	27.22	27.465
	T_{cond} (bubble) [°C]	136.76	136.77	136.81	136.83
	Ref-side pressure drop [kPa]	0.087	0.088	0.0906	0.092
Subcooler	Capacity [kW]	24.779	22.813	20.989	18.905
	Total subcooling [K]	69.871	63.322	56.773	50.109
	Ref-side pressure drop [kPa]	3.0346	3.055	3.106	3.136
Evaporator	Capacity [kW]	43.893	42.068	40.603	38.725
	T_{evap} (dew) [°C]	74.657	74.84	75.303	75.566
	Ref-side pressure drop [kPa]	5.542	5.956	6.687	7.17
Global Performance	Total heat provided [kW] (condenser + subcooler)	51.402	49.605	48.209	46.370
	COP_{HTHP} [-]	4.931	4.741	4.566	4.370

6. Conclusions

The current deliverable summarizes the steps of sizing, selecting, and assessing the different components for a HTHP laboratory prototype as a part of CHEST system in the range of 10 kWe. Different parametric studies were implemented to study the HTHP performance under different working conditions. Furthermore, the control and operation strategies for the proposed HTHP were discussed.

R-1233zd(E) was selected as candidate for the subcritical HTHP prototype due to many advantages such as low-GWP (<1), non-toxic and non-flammable fluid (A1), high critical temperature (166.5 °C), and no need for high SH (isotropic fluid).

The EES-CHEST model, adopting R-1233zd(E) as the working fluid for both HTHP and ORC, estimated a roundtrip efficiency (ratio between net power output from ORC to the power input to the HTHP) of 0.74 when the HTHP's source temperature= 100 °C, PCM melting temperature= 133 °C, and ORC's sink temperature= 25 °C. This indicates that CHEST concept is very promising technology for storing and managing the thermal energy.

Based on EES-CHEST system results the maximum capacities for HTHP's components were specified, and then each component was sized and selected. The selected compressor is single piston compressor with maximum rpm of 1500 and swept volume=511 cm³ (from Viking heat engines). Regarding heat exchangers, they were selected based on SWEP SSP G8 selection tool. The evaporator has 60 plates with 7.66 m² heat transfer area, the condenser has 106 plates with 13.4 m² heat transfer area, and, finally, the subcooler has 62 plates with heat transfer area of 3.6 m².

Different parametric studies were implemented by IMST-ART[®] simulation tool to define the limits and assess the performance of proposed HTHP for different compressor speeds, source temperatures, and inlet water temperatures for subcooler. Under the nominal point (source temperature= 85 °C, compressor speed= 1500 rpm, HTHP's sink temperature= 133 °C), the estimated COP of HTHP was 4.86 for total heat provided of 50.68 kW and input power of 10.43 kW.

References

- [1] "CHESTER (Compressed Heat Energy STORAGE for Energy from Renewable sources) Project." [Online]. Available: <https://www.chester-project.eu/>. [Accessed: 14-Feb-2019].
- [2] C. Pascual, "D2.4 Requirements of individual technologies that form the CHESTER system," Bizkaia, Spain, 2019.
- [3] H. Jockenhöfer, W. D. Steinmann, and D. Bauer, "Detailed numerical investigation of a pumped thermal energy storage with low temperature heat integration," *Energy*, vol. 145, pp. 665–676, 2018.
- [4] C. Arpagaus, F. Bless, M. Uhlmann, J. Schiffmann, and S. S. Bertsch, "High temperature heat pumps: Market overview, state of the art, research status, refrigerants, and application potentials," *Energy*, vol. 152, pp. 985–1010, 2018.
- [5] S. A. Klein, "Engineering Equation Solver (Version V10.643)." F-Chart Software, 2019.
- [6] E. W. Lemmon, I. H. Bell, M. L. Huber, and M. O. McLinden, "NIST Standard Reference Database 23: Reference Fluid Thermodynamic and Transport Properties-REFPROP." National Institute of Standards and Technology, Gaithersburg, 2018.
- [7] ASHRAE, "Standard 34-safety standard for refrigeration systems and designation and classification of refrigerants.," 2016.
- [8] J. M. Corberán, A. H. Hassan, and J. Payá, "Thermodynamic analysis and selection of refrigerants for high-temperature heat pumps," in *Proceedings of the 25th IIR International Congress of Refrigeration*, 2019.
- [9] T. Fleckl, M. Hartl, F. Helminger, and K. Kontomaris, "Performance testing of a lab-scale high temperature heat pump with HFO-1336mzz-Z as the working fluid," in *European Heat Pump Summit 2015, October 20-21.*, 2015.
- [10] Viking Heat Engines, "HeatBooster." [Online]. Available: <http://www.vikingheatengines.com/heatbooster>.
- [11] O. Bamigbetan, T. M. Eikevik, P. Nekså, M. Bantle, C. Schlemminger, and M. Dallai, "Experimental investigation of a hydrocarbon piston compressor for high temperature heat pumps," *24th Int. Compress. Eng. Conf. Purdue, July 9-12, 2018*, no. August, pp. 1–9, 2018.
- [12] IMST-ART, "Simulation Tool to Assist the Selection, Design and Optimization of Refrigeration Equipment and Components," *Instituto Universitario de Investigación en Ingeniería Energética, Universitat Politècnica de València, Valencia*, 2010. [Online]. Available: <http://www.imst-art.com/>.
- [13] J. M. Corberan and J. Gonzalez, "A computer code to assist the design of refrigeration and A/C equipment," in *Purdue Refrigeration Conference, West Lafayette, Indiana, USA*, 2002.
- [14] J. M. Corberán, P. F. De Córdoba, J. González, and F. Alias, "Semiexplicit method for wall temperature linked equations (SEWTLE): A general finite-volume technique for the calculation of complex heat exchangers," *Numer. Heat Transf. Part B Fundam.*, vol. 40, no. 1, pp. 37–59, 2001.
- [15] SWEP International AB, "SWEP SSP G8 (V. 2019.619.2.0)." 2019.

Annex

A.1. HTHP's Evaporator detailed specifications and dimensions:

Model: SWEP V120THx60/1P			
		Side 1: R-1233zd(E)	Side 2: water
Flow direction	-	Counterflow	
Capacity	kW	62.25	
Mass flow	kg/s	0.4	3.6
Total heat transfer area	m ²	7.66	
Heat flux	kW/m ²	8.13	
Overall heat transfer coefficient	W/m ² .K	1024	
Pressure drop (Total)	kPa	10.4	32.5
Number of plates	-	70	
Dimensions (HxWxL)	mm	525x243x148	

A.2. HTHP's condenser detailed specifications and dimensions:

Model: SWEP B200THx106/1P			
		Side 1: R-1233zd(E)	Side 2: water
Flow direction	-	Counterflow	
Capacity	kW	44.8	
Mass flow	kg/s	0.4	10.5
Total heat transfer area	m ²	13.4	
Heat flux	kW/m ²	3.34	
Overall heat transfer coefficient	W/m ² .K	738	
Pressure drop (Total)	kPa	-0.6	64
Number of plates	-	106	
Dimensions (HxWxL)	mm	525x243x253	

A.3. HTHP's subcooler detailed specifications and dimensions:

Model: SWEP B86Hx62/1P			
		Side 1: R-1233zd(E) (liquid)	Side 2: water
Flow direction	-	Counterflow	
Capacity	kW	41.4	
Mass flow	kg/s	0.4	0.11
Total heat transfer area	m ²	3.6	
Heat flux	kW/m ²	11.5	
Overall heat transfer coefficient	W/m ² .K	978	
Pressure drop (Total)	kPa	4	0.4
Number of plates	-	62	
Dimensions (HxWxL)	mm	526x119x108	